Chem Soc Rev

CHIRALITY IN CURVED POLYAROMATIC SYSTEMS

Chirality in curved polyaromatic systems

Michel Rickhaus,[ab] Marcel Mayor*[acd] and Michal Juríček[a]

[a] Department of Chemistry, University of Basel, St. Johanns-Ring 19, 4056 Basel, Switzerland.
E-mail: marcel.mayor@unibas.ch

[b] Department of Chemistry, University of Oxford, Chemistry Research Laboratory, Mansfield Road, OX1 3TA Oxford, United Kingdom

[c] Institute for Nanotechnology (INT), Karlsruhe Institute of Technology (KIT), P. O. Box 3640, 76021 Karlsruhe, Germany

[d] Lehn Institute of Functional Materials (LIFM), Sun Yat-Sen University, Guangzhou, P. R. China

Chem Soc Rev

TUTORIAL REVIEW

Table of contents

Chiral non-planar polyaromatic systems that display zero, positive or negative Gaussian curvature are analysed and their potential to 'encode' chirality of larger sp^2-carbon allotropes is evaluated. Shown below is a hypothetical peanut-shaped carbon allotrope, where helical chirality results from the interplay of various curvature types.
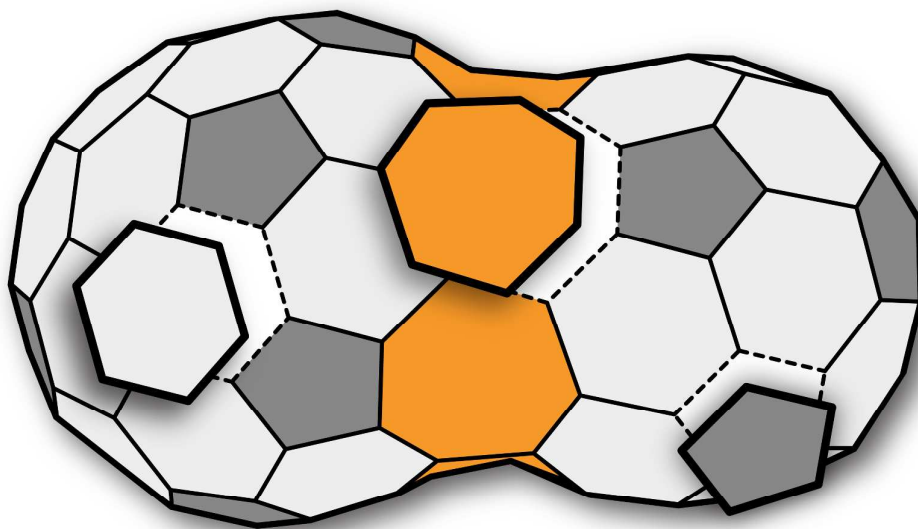
Abstract

Carbon allotropes constituted of sp^2-hybridised carbon atoms display a variety of properties that arise from their delocalised π-conjugated electronic structure. Apart from carbon's planar allotropic form graphene, bent or curved structures, such as carbon nanotubes or fullerenes, respectively, have been discovered. In this Tutorial Review, we analyse and conceptually categorise chiral synthetic molecular fragments of non-planar sp^2-carbon allotropes, including hypothetical forms of carbon that have been proposed to exist as stable entities. Two types of molecules composed of equally or differently sized rings are examined: *bent* with zero Gaussian curvature and *curved* with positive or negative Gaussian curvature. To affirm that a system is chiral, two conditions must be fulfilled: (1) both reflective symmetry elements, an inversion centre and a mirror plane, must be absent and (2) the system must be stereochemically rigid. It is therefore crucial to not only consider the symmetry of a given system as if it was a rigid object but also its structural dynamics. These principles serve as guidelines for the design of molecular fragments that encode and transcribe chirality into larger systems.

Key learning points

1. Non-planar sp^2-carbon allotropes and their molecular fragments can display zero, positive or negative Gaussian curvature.

2. 'Tubes' obtained by bending of a planar hexagonal sheet display zero Gaussian curvature.

3. Non-zero Gaussian curvature arises when non-hexagonal rings are introduced in the hexagonal sp^2-carbon lattice to afford 'bowls' and 'saddles'.

4. The first requirement for tubes, bowls and saddles to be chiral is the absence of reflective symmetry elements, namely, an inversion centre and a symmetry plane.

5. The second requirement is that a chiral system must be stereochemically rigid and separable into enantiomers under ambient conditions.

1. Introduction

Carbon is the most diverse element in the periodic table in terms of its unrivalled ability to form an infinite number of structures, which is reflected by the structural diversity of known carbon allotropes. Carbon allotropes[1] made exclusively of sp^2-hybridised carbon atoms are of particular interest, on account of their delocalised π-conjugated electronic structure and an array of properties—related to charge transport, light absorption and emission, or magnetism—which differ distinctly allotrope to allotrope. An archetypal example of sp^2-carbon allotropes is graphene (Fig. 1a), a single sheet of graphite, in which sp^2-hybridised carbon atoms are arranged such that they form a two-dimensional hexagonal lattice composed of fused benzenoid rings.

Bending a planar sheet of graphene into a seamless three-dimensional tube results in a cylindrical structure—termed carbon nanotube[2]—which similarly to graphene consists solely of fused benzenoid rings. Depending on the way that a graphene sheet is bent into a tube with respect to its lattice unit vectors (a_1 and a_2), chiral carbon nanotubes (Fig. 1b) can be conceptualised in addition to two achiral forms, armchair and zigzag. A special feature of carbon nanotubes is that they can be metallic or semiconducting, and this distinctive behaviour is dictated solely by the 'bending mode', which directly relates conductivity to chirality. The case of carbon nanotubes illustrates beautifully how a simple operation such as bending of a graphene sheet can give origin to *chirality* and the impact of chirality on the electronic structure and the resultant properties of sp^2-carbon allotropes. Because chiral sp^2-carbon allotropes contain stereogenic axes and not stereogenic centres, they can be categorised as axially (helically) chiral.
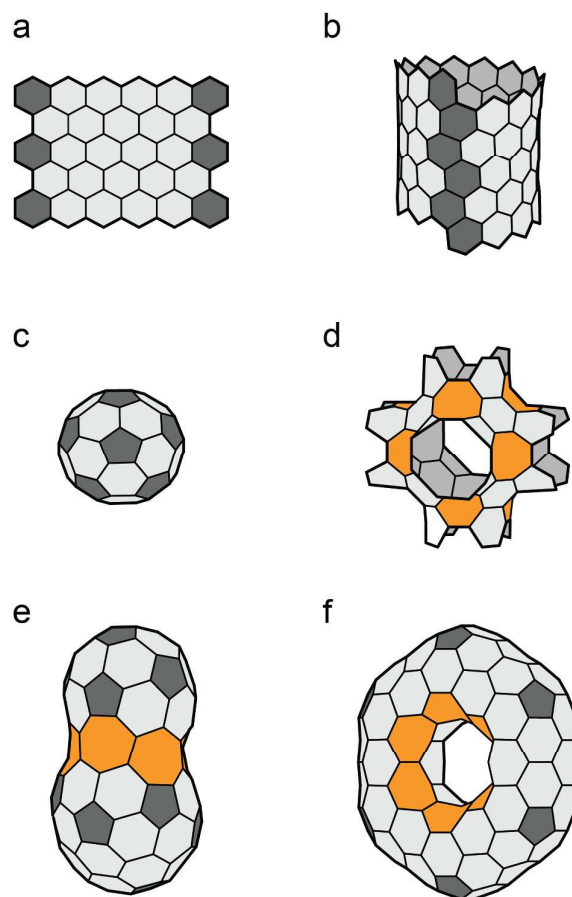
Fig. 1 Schematic illustrations of sp^2-carbon allotropes: (a) graphene and (b) carbon nanotube segments with zero Gaussian curvature, (c) fullerene with positive Gaussian curvature, (d) unit cell of a schwarzite with negative Gaussian curvature and (e) fullerene dimer and (f) toroidal carbon nanotube with different curvature types. Structures in (a–c) are known, hypothetical structures in (d–f) have been predicted to exist as stable entities and structures in (b) and (e) are chiral. Colour code for n-membered rings: dark gray (n = 5), light gray (n = 6) and orange (n = 7 or 8). Six-membered rings in (a) and (b) that highlight the 'sewing' section are coloured in dark gray. Double bonds are omitted for clarity.

In addition to sp^2-carbon sheets comprising exclusively six-membered rings and tubes made by *bending* of these sheets, *curved* three-dimensional structures[1] are possible if other than six-membered rings are introduced in the hexagonal sp^2-carbon lattice. These structures display positive ('bowls') or negative ('saddles') Gaussian curvature in contrast to sheets and tubes, which both represent a surface of zero Gaussian curvature (Fig. 2).

a	b	c
zero curvature	positive curvature	negative curvature
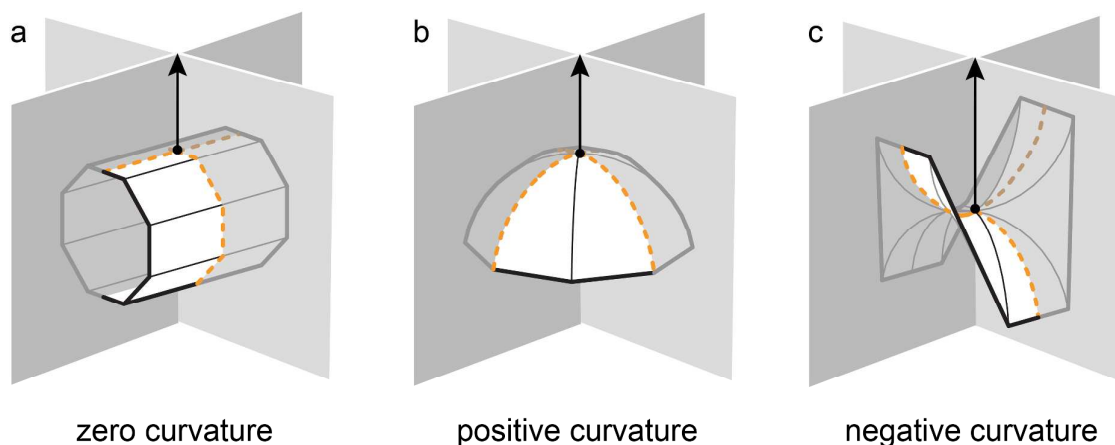
Fig. 2 Schematic illustration of three different types of Gaussian curvature: (a) zero, (b) positive and (c) negative. In differential geometry, the Gaussian curvature (K) of a surface at a point (black dot) is the product of the principal curvatures, κ_1 and κ_2, at this point: $K = \kappa_1\kappa_2$. The principal curvatures are by definition the maximum and minimum curvatures of normal sections. A normal section is an intersection (dashed orange line) between the surface and a normal plane (in gray), which is any plane that contains a vector that is at right angles to the surface (normal vector, black arrow). According to equation $K = \kappa_1\kappa_2$: if one of the principal curvatures is zero, then $\kappa_1\kappa_2 = 0$ and the Gaussian curvature is denoted zero, if both principal curvatures have the same sign, then $\kappa_1\kappa_2 > 0$ and the Gaussian curvature is denoted positive and if the principal curvatures have opposite signs, then $\kappa_1\kappa_2 < 0$ and the Gaussian curvature is denoted negative. Tube-, bowl- and saddle-shaped molecules discussed in this review display zero, positive and negative curvature, respectively, however, some molecules can display multiple types of curvature at different points (see, for example, toroidal nanotube structure in Fig. 1f).

Spherical sp^2-carbon allotropes, known as fullerenes, display positive curvature induced by five-membered rings (Fig. 1c), while negative curvature is featured in schwarzites, or carbon 'foams', a theoretical type of sp^2-carbon allotropes proposed[3] by Mackay and Terrones, which contain seven- or eight- in addition to six-membered rings (Fig. 1d). An even more exotic surface topology is found in hypothetical toroidal carbon nanotubes[4] comprising five-, six-, and seven-membered rings, which display positive curvature on the outside and negative curvature on the inside of the torus, and zero curvature in between the two curved segments (Fig. 1f). A chiral example of a curved sp^2-carbon allotrope is a fullerene dimer inspired by structures proposed[5] by Diudea, in which two fullerene

subunits are fused via a 'belt' formed by fused seven-membered rings. This peanut-shaped molecular allotrope features positively and negatively curved segments, which are merged in a unique manner and yield an unprecedented helically twisted curved geometry (Fig. 1e).

Although sp^2-carbon allotropes such as graphene and carbon nanotubes have formally infinite and highly regular structures, in reality they are finite molecules, which may or may not contain structural defects. Their bulk preparation relies mostly on synthetic methods that are difficult to control, often require harsh reaction conditions and lead to inseparable mixtures of differently sized and edged molecules, which display a combination of properties. Because understanding the structure–property relationship of 'single molecules' is crucial for the development of new carbon materials as well as their potential applications, there is a need for structurally 'pure' and monodispersed molecules, which have so far only been accessed in the case of fullerenes. The most promising approach to structurally uniform sp^2-carbon allotropes takes advantage of small molecules[6] that 'encode' structural information of the respective allotropes and act[7] as building blocks for polymerisation. This strategy could deem successful for the preparation of schwarzite and other hypothesised sp^2-carbon allotropes that should according to computational predictions exist as stable entities. The chemistry of sp^2-carbon-allotrope fragments, which could serve as monomers for building larger structures, continue to attract interest of synthetic chemists and the fruits of the enormous efforts dedicated to make such molecular building blocks have been reviewed[1,2,6] in recent years on several occasions. In this Tutorial Review, we systematically analyse the interplay between the structure of these molecules and chirality. It is important to note that this conceptual study deals with *skeletal chirality*, that is, helical chirality of the fused polyaromatic cores of sp^2-carbon allotrope fragments and does not include skeletally achiral molecules where chirality is achieved by other means, such as peripheral substitution or heteroatom-doping.

In our previous review on chiral polyaromatic systems,[8] we conceptually categorised skeletally chiral molecular fragments of planar sp^2-carbon allotrope graphene, or 'nanographenes', in which steric interactions between rings or substituents in close proximity that are present in their planar form

induce helical twist of the polyaromatic system. Here, we analyse and categorise chiral molecular fragments of non-planar sp^2-carbon allotropes that display zero, positive or negative Gaussian curvature induced by strain that arises from lattice defects. The known examples from the literature are divided into two classes with regards to the type of non-planar surface they represent (Fig. 2): *bent* systems with zero Gaussian curvature (a, tubes) described in Section 2 and *curved* systems with positive (b, bowls) or negative (c, saddles) Gaussian curvature described in Section 3. Chirality of these systems is analysed with respect to the symmetry of their three-dimensional structures as well as in consideration of their stereochemical rigidity/dynamics, in accord with the IUPAC rules. In terms of symmetry, the analysed structures are divided into two types, depending on whether they possess at least one reflective symmetry element (RSE), an inversion centre (*i*) or a symmetry plane (*σ*), or not (no RSE). In terms of stereochemical rigidity/dynamics, the analysed molecular fragments are classified as either (a) stereochemically rigid, when the isomerisation barrier (roughly >20 kcal mol^{-1}) allows for a preparative isolation of individual stereoisomers under ambient conditions, (b) stereochemically non-rigid, when the isomerisation barrier (roughly 5–20 kcal mol^{-1}) does not allow for a preparative isolation of individual stereoisomers under ambient conditions, but allows for their observation by an experimental technique such as NMR within a practical temperature range and (c) stereochemically fluctuating, when the isomerisation barrier (roughly <5 kcal mol^{-1}) does not allow for an experimental observation of individual stereoisomers. In this context, a molecule is considered to be chiral if and only if (1) it does not possess any RSEs and (2) it is stereochemically rigid. Note that some chiral compounds do undergo racemisation under ambient conditions, however, the racemisation process is sufficiently slow to allow for the preparative separation and isolation of the corresponding enantiomers. In addition, we discuss the relationship of these molecular fragments to one or more sp^2-carbon allotropes, the structural information, but not necessarily the chiral information, of which they 'encode'. It is important to note that this relationship is not discussed in order to define chirality of these fragments, but to illustrate whether their chirality can be transcribed into a chiral sp^2-carbon allotrope or not.

The real examples of different types of chiral polyaromatic curved systems are discussed in detail in the following sections. We carefully selected illustrative examples with the aim to conceptualise design principles that lead to chiral polyaromatic systems that represent fragments of sp^2-carbon allotropes rather than giving an exhaustive overview. Compounds, for which the solid-state structures as well as the Gibbs free energy barriers ($\Delta G_T^{\ddagger}$) of racemisation are available, were selected preferentially. In cases when solid-state structures were not available, optimised geometries (DFT/B3LYP/6-31G(g,d)) were used instead. The CCDC numbers for the solid-state structures used in this review are listed at the end of this manuscript for the reader's convenience and the optimised geometries are provided as Electronic Supplementary Information (ESI) files (PDB). We hope that our analysis of chirality in curved polyaromatic systems will motivate further research in this field and find use in design and construction of new structurally uniform allotropic forms of carbon that are chiral.

2. Chirality in systems with zero Gaussian curvature

Bending a planar sheet of graphene into a seamless rigid tube results in a formally infinite cylindrical structure that displays zero Gaussian curvature, featured by sp^2-carbon allotropes known[2] as carbon nanotubes (CNTs). Depending on the mode of bending, CNTs that either do (achiral) or do not (chiral) contain reflective symmetry elements (RSEs) can be obtained, which is schematically illustrated in Fig. 3, where an orange-filled, black-striped rectangular sheet represents graphene. It is important to note the difference between these two distinct modes of bending with regards to a defect-free π-extension, that is, extension with six-membered rings only and retaining the zero Gaussian curvature. A chiral tube can only be extended into a longer chiral tube. In contrast, an achiral tube can be extended into a chiral one, if such extension reduces the symmetry of the resulting tube. Additionally, such a chiral tube obtained by extension of an achiral tube can be further extended into an achiral tube. In analogy to the concept of prochirality in stereochemistry, an achiral tube can be regarded as 'prochiral', as its extension (or subtraction) can provide a chiral

structure. Turning a planar system into a non-planar one (bent or curved) can therefore be regarded as a process that induces prochirality.
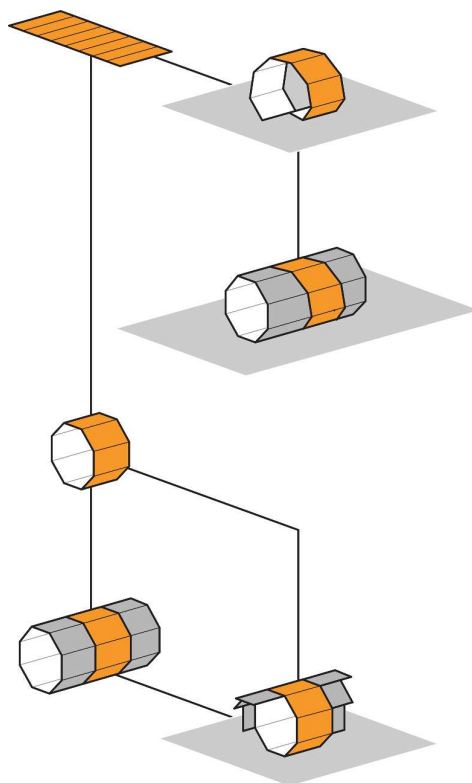
Fig. 3 *Schematic illustration of bending of a planar sheet (orange, top left) into a chiral and an achiral rigid tube segment. Chiral tube segment can only be extended into a chiral tube segment, while achiral tube segment can be extended into a chiral tube segment or an achiral one. Parent segments are highlighted in orange, extensions are shown in gray and chiral tube segments are marked with gray underlying squares/rectangles.*

The structure of a CNT is described by a diameter (typically ranging from one to tens of nanometres), length (typically of up to centimetres), and a vector (C_h) along which a sheet of graphene is bent with respect to its two unit vectors a_1 and a_2. The C_h vector is defined as $C_h = na_1 + ma_2$ (Fig. 4b), where indices n and m are integers, and the corresponding CNT is named by using a prefix (n,m). Depending on indices n and m, three types of CNTs can be conceptualised (Fig. 4a, top): achiral armchair ($n = m$) and zigzag ($m = 0$), and chiral ($n \neq m$). In contrast to graphene, which is a two-dimensional

semimetal, CNTs can be[1,2] either metallic (armchair), semiconducting with a very small band gap (chiral with $n - m$ = multiple of 3), or moderately semiconducting (all other types) along the main axis. This unique structure–property relationship, which relates to chirality, underlies the need for chiral structurally uniform CNTs. Because the chemical properties of CNTs are very similar, which hampers the separation of monodispersed species, suitable molecular building blocks encoding the key structural features are needed for their bottom-up construction.

The smallest ring fragments of CNTs known[2] as carbon 'nanorings' or 'nanohoops' are formally obtained by 'slicing' of CNTs. They have a cyclic structure formed by arylene units (*e.g.*, paraphenylene) linked via single bonds and represent the thinnest polyaromatic slices of CNTs (Fig. 4a, bottom). Molecular analogues of carbon nanorings are [*n*]cycloparaphenylenes ([*n*]CPPs) for armchair (*n*,*n*)-CNTs and [*n*]cyclometaphenylenes ([*n*]CMPs) for zigzag (*n*,0)-CNTs. In the case of chiral CNTs, one possible type of nanoring fragments are C[n_1]PP[n_2]A molecules[9] that feature one [n_1]paraphenylene ([n_1]PP) and one [n_2]acene ([n_2]A) segment linked together forming a cycle. By using indices n_1 and n_2, the corresponding chiral CNT is defined as ($n_1 + n_2$, $n_1 + 1$). For example, a nanoring featuring one [5]PP (dark gray) and one 2,6-naphthylene ([2]A, orange) segment is a fragment of (7,6)-CNT (Fig. 4a, right). Fragments of CNTs that comprise only fused benzenoid rings and do not contain single-bond linkages are known[2] as carbon 'nanobelts'. The thinnest possible nanobelt fragments of armchair, zigzag and chiral CNTs are shown in Fig. 4a, middle. From a stereochemical view, a clear distinction between nanobelts and nanorings must be made. Nanobelts are rigid molecules with a persistent cylindrical shape of CNTs, while nanorings are typically non-rigid/fluctuating molecules, which undergo rapid interconversion between all possible conformations under ambient conditions. As a result, nanobelts that do not contain any RSEs are by definition chiral and nanorings achiral. There are, however, exceptions to this rule and stereochemically rigid nanorings that are chiral have been achieved (see below).
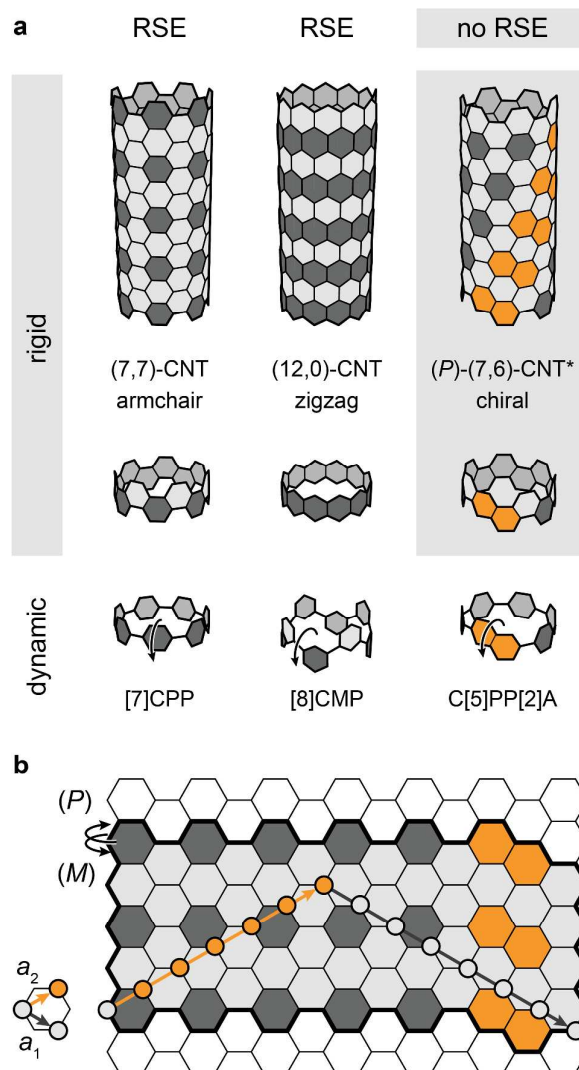
Fig. 4 (a) Schematic illustration of three types of carbon nanotubes (CNTs, top) and their nanobelt (middle) and nanoring (bottom) fragments: armchair (left), zigzag (centre) and chiral (right). In contrast to CNTs and nanobelts, which are stereochemically rigid, nanorings that contain single-bond linkages are dynamic (i.e., stereochemically non-rigid/fluctuating; the non-restricted rotation of the arylene units around two single bonds in nanorings is illustrated with an arrow). Chiral systems, that is, rigid systems that do not possess any reflective symmetry elements (RSEs), are highlighted with a gray background and an asterisk next to the name. Absolute configuration of (P)-(7,6)-CNT was determined according to previously proposed[12] rules. (b) Chiral (P)-(7,6)-CNT shown in (a) was obtained by bending of the respective graphene fragment into a tube with respect to a vector $C_h = 7a_1 + 6a_2$. The (M)-enantiomer of this CNT can be obtained by bending the same sheet in the opposite direction (see the arrows). a_1 and a_2 are the lattice unit vectors of graphene. Colour code: benzenoid

rings (light/dark gray), 2,6-naphthylene units of C[5]PP[2]A fragments (orange). Double bonds are omitted for clarity.

The reason for the non-rigid/fluctuating character of nanorings is the presence of single-bond linkages. Similarly to biaryl systems, the non-coplanar orientation of each pair of neighbouring arylene units in nanorings is favoured over the planar one, on account of steric repulsion between hydrogen atoms in *ortho*-positions, which can give rise to conformations that do not contain any RSEs. Because, however, the barrier of rotation around single bonds is low, the arylene units can 'freely' rotate under ambient conditions and the individual stereoisomers cannot be isolated. In biphenyl systems, restricted rotation (high energy barrier, no rotation under ambient conditions) can be achieved by instalment of bulky *ortho*-substituents. In the case of cyclic systems such as nanorings, restricted rotation can also arise on account of strain that increases with decreasing the size of the nanoring and/or increasing the size of the arylene unit, as discussed below.

Nanorings C[n_1]PP[n_2]A represent fragments of chiral ($n_1 + n_2$, $n_1 + 1$)-CNTs. Itami and co-workers synthesised[9] the first and so far the only nanoring of this type, namely, C[13]PP[2]A (in the original publication denoted as [13]CPPN, 'N' for naphthalene), a fragment of (15,14)-CNT. According to DFT calculations, the most stable conformation of C[13]PP[2]A does not possess any RSEs. Because of fast rotation of the naphthylene unit around two single bonds, however, the compound cannot be resolved into its enantiomers at room temperature. The Gibbs free energy barrier ($\Delta G_T^{\ddagger}$) of this rotation process estimated by DFT calculations (B3LYP/6-31G(d)) has a value of 8.4 kcal mol^{-1}, meaning that C[13]PP[2]A is stereochemically non-rigid and thus achiral. To aid the design of C[n_1]PP[n_2]A nanorings, where rotation of the [n_2]A unit is restricted, Itami computationally investigated[9] the rotational barriers of other homologues in this series, namely, C[n_1]PP[n_2]As with n_1 ranging from 5 to 13 and n_2 ranging from 2 to 4. A general trend was found across the series: the rotational barriers increase (i) with a decreasing number (n_1) of phenylene rings, that is, a decreasing size of nanoring, and (ii) with an increasing number (n_2) of benzenoid rings in the acene unit. The highest energy barriers were obtained for C[5]PP[3]A (45.5 kcal mol^{-1}), C[6]PP[4]A (44.0 kcal mol^{-1}),

C[7]PP[4]A (33.0 kcal mol^{-1}), C[6]PP[3]A (31.3 kcal mol^{-1}) and C[5]PP[2]A (29.6 kcal mol^{-1}). According to these values, these compounds should be stereochemically rigid and thus separable into enantiomers under ambient conditions. Additionally, ring-strain energies estimated for all compounds revealed that even the smallest rings such as C[5]PP[2]A (ring-strain energy of 89.9 kcal mol^{-1}) should exist as stable molecules.

Stereochemically rigid nanorings have recently been synthesised[10–12] by Isobe and co-workers, who linked via single bonds four chrysenylene ([4]CC[11,12]) and four anthanthrenylene ([4]CA[10]) units into a cycle. Rotation of the arylene units around single bonds in these systems affords different rotational conformers (rotamers), which differ by relative orientations of the arylene units (Fig. 5). Similarly to [n]CPPs, the arylene units adopt non-coplanar relative orientations with an average torsion-angle value in the range of ~18–38° (Fig. 5e), as estimated by DFT calculations[12] and X-ray diffraction[11] (XRD) analysis. Because rotation through the ~0° and ~180° torsional points has lower energy barrier than rotation through the ~90° and ~270° torsional points, E/Z formalism was introduced[10–13] by Isobe and co-workers to describe the relative orientation of each pair of arylene units (Fig. 5). Unlike in [n]CPPs and C[n_1]PP[n_2]As, however, the energy barrier of an '(E)-to-(Z)' rotation in [4]CCs and [4]CAs is relatively high, as a result of the large size of the arylene blocks (relative to phenylene). The high energy barrier of rotation allowed Isobe and co-workers to separate and isolate on a preparative scale all possible rotamers that relate to one another either as enantiomers or diastereomers. Remarkably, the high rotational barrier in these systems arises solely on account of ring strain, in contrast to acyclic biaryl systems, where *ortho*-substituents are crucial for restricting rotation around the aryl–aryl single bonds.

Two types of [4]CCs were synthesised to date, one with a 2,8- ([4]CC$_{2,8}$)[12] and one with a 3,9- ([4]CC$_{3,9}$)[11] linkage pattern. In both cases, six stereoisomers are possible, namely, four diastereomers, two of which are achiral and the other two exist as pairs of enantiomers. The six possible stereoisomers for [4]CC$_{2,8}$ or [4]CC$_{3,9}$ are: (P)-(E,E,E,E), (M)-(E,E,E,E), (P)-(E,E,Z,Z), (M)-(E,E,Z,Z), (E,Z,E,Z), and (Z,Z,Z,Z). The most unique feature of the [4]CC systems is that different

13

diastereomers represent[12] different nanoring fragments of CNTs. In the case of [4]CC$_{2,8}$, the first reported type, the chiral (*E,E,E,E*)- and (*E,E,Z,Z*)-isomers (Fig. 5c,d) are fragments of chiral CNTs, (12,8) and (11,9), respectively, while achiral (*E,Z,E,Z*)- and (*Z,Z,Z,Z*)-isomers (Fig. 5b) both represent fragments of achiral armchair (10,10)-CNT.
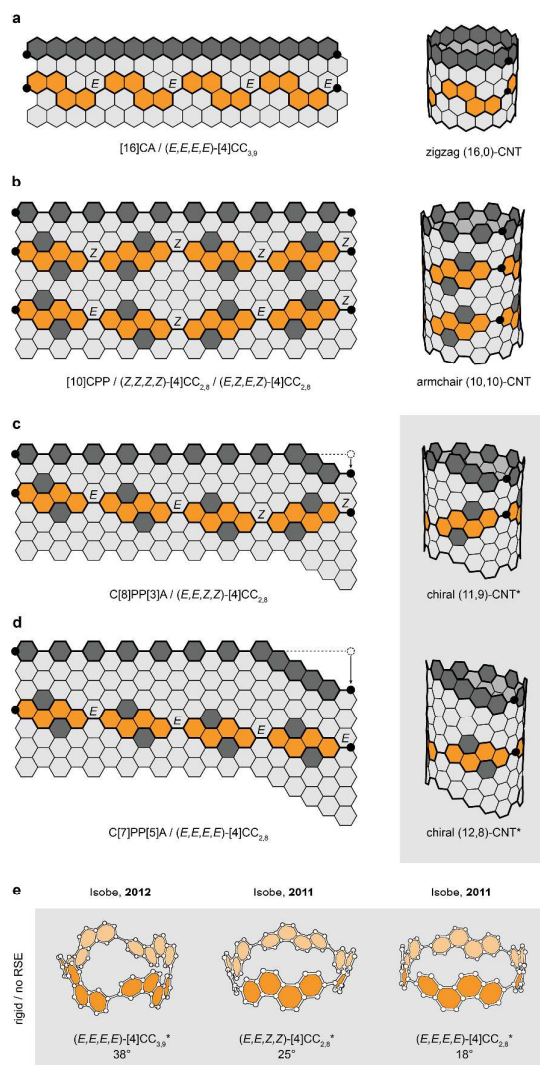
Fig. 5 *(a–d) Schematic representation of graphene fragments (left) that upon bending and fusing of left and right edges afford finite tubular fragments of CNTs (right): (a) zigzag (16,0), (b) armchair (10,10), (c) chiral (11,9) and (d) chiral (12,8). The basic nanoring unit of each CNT fragment is highlighted in dark gray on top of each sheet: (a) [16]CA, (b) [10]CPP, (c) C[8]PP[3]A and (d) C[7]PP[5]A. The [4]CC$_{3,9}$ (a) and [4]CC$_{2,8}$ (b–d) nanoring units are highlighted in orange and the [4]CA$_{2,8}$ (b–d) nanoring units are represented by a combination of orange and dark gray. The relative*

orientation of the arylene units around each single bond is denoted by descriptors E and Z. Double bonds are omitted for clarity. Selected pairs of the edge carbon atoms, one on the left and one on the right, that get fused when forming the tube are highlighted by black-filled circles. The black-filled circles on the left are shown on the right at the same vertical level as dotted-line circles for easier visualisation of the vertical offset. This offset is constant for each nanoring fragment of the same CNT. Enantiomers of [4]CC and [4]CA fragments in (b–d) are obtained by bending of the sheet in opposite directions (see Fig. 4b). (e) Solid-state structure of (E,E,E,E)-[4]CC$_{3,9}$ (XRD) and optimised geometries of (E,E,Z,Z)-[4]CC$_{2,8}$ and (E,E,E,E)-[4]CC$_{2,8}$ (DFT). The average torsion-angle value for relative orientations between the chrysenylene units is given. (a–e) Chiral systems, that is, rigid systems that do not possess any reflective symmetry elements (RSEs), are highlighted with a gray background and an asterisk next to the name.

In the case of [4]CC$_{3,9}$ reported[11] later by the same group, the chiral (*E,E,Z,Z*)-isomer is a fragment of chiral (12,4)-CNT, while the achiral (*E,Z,E,Z*)- and (*Z,Z,Z,Z*)-isomers are both fragments of achiral armchair (8,8)-CNT and, notably, the chiral (*E,E,E,E*)-isomer (Fig. 5a) is a fragment of achiral zigzag (16,0)-CNT. Interestingly, all six stereoisomers formed[12] during the synthesis of [4]CC$_{2,8}$, while only the (*E,E,E,E*)-isomer formed[11] in the case of [4]CC$_{3,9}$. In both cases, all formed stereoisomers could be separated and isolated as pure compounds. (*E,E,E,E*)-[4]CC$_{3,9}$ is the first fragment of a zigzag CNT synthesised to date, as the nanobelt fragments of zigzag CNTs, [*n*]cyclacenes, have not yet been synthesised despite numerous efforts dedicated to their bottom-up preparation.
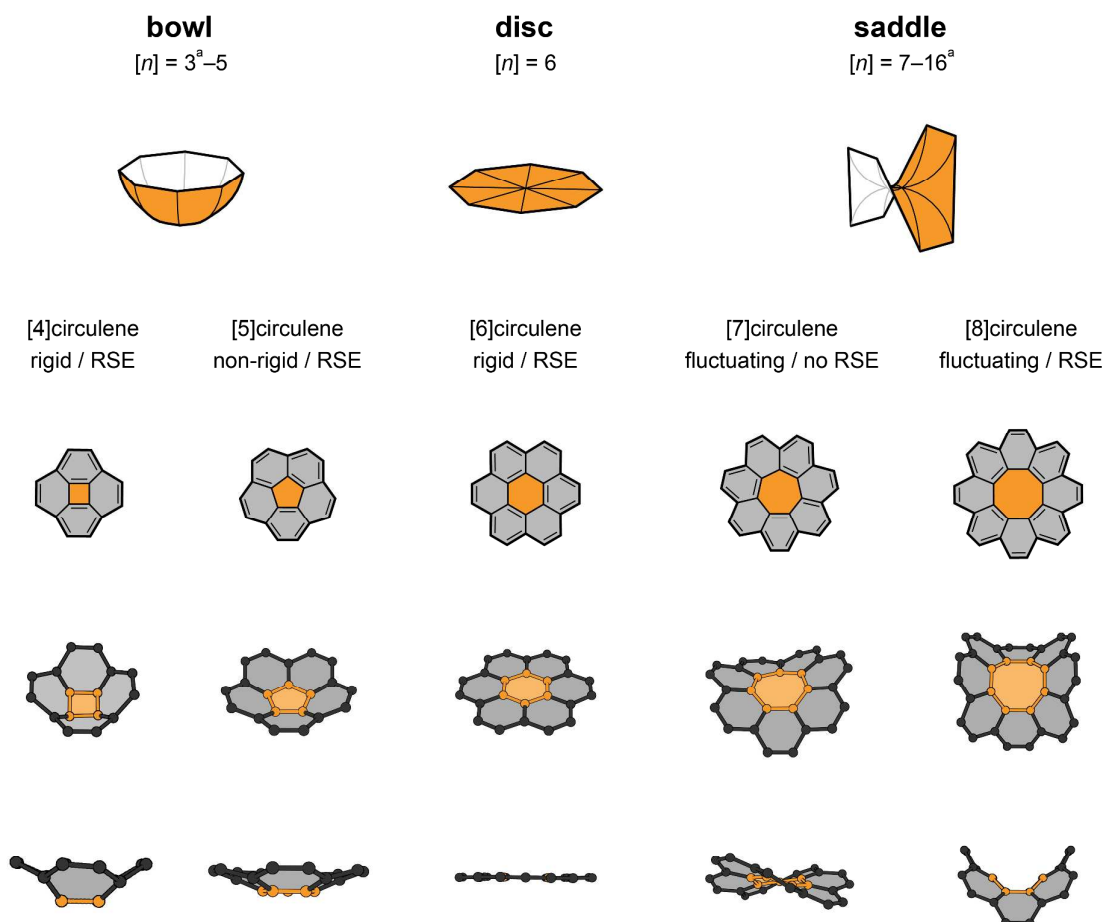
The presence of single bonds in [4]CCs gives rise to an interesting dynamics[10] related to rotation of the chrysenylene units around these single bonds. It was found that the stereoisomers can interconvert to one another in a stepwise process that occurs via rotation of one chrysenylene unit at a time. For example, (*P*)-(*E,E,E,E*)-[4]CC$_{2,8}$ is first converted to (*P*)-(*E,E,Z,Z*)-[4]CC$_{2,8}$ upon rotation of one chrysenylene unit, and (*P*)-(*E,E,Z,Z*)-[4]CC$_{2,8}$ is then transformed to either (*E,Z,E,Z*)- or (*Z,Z,Z,Z*)-[4]CC$_{2,8}$ upon rotation of a second chrysenylene unit. Both (*E,Z,E,Z*)- or (*Z,Z,Z,Z*)-[4]CC$_{2,8}$ are subsequently converted to (*M*)-(*E,E,Z,Z*)-[4]CC$_{2,8}$, which is finally transformed to (*M*)-(*E,E,E,E*)-[4]CC$_{2,8}$. In accord with this mechanism, a complete equilibration leading to a thermodynamic mixture of all possible isomers occurred upon heating a solution of (*P*)-(*E,E,E,E*)-[4]CC$_{2,8}$ at 353 K for

50 h. By using an Eyring plot of the temperature-dependent decay of (*P*)-(*E,E,E,E*)-[4]CC$_{2,8}$, the energy barrier of rotation was estimated[10] for the [4]CC$_{2,8}$ system (333–453 K): $\Delta H^{\ddagger}$ = +26 kcal mol^{-1} and $\Delta S^{\ddagger}$ = +5.2 cal K^{-1} mol^{-1} ($\Delta G_{393}{}^{\ddagger}$ = +24 kcal mol^{-1}). The calculated (DFT/B3LYP/6-31(d,p)) energy barrier of rotation (29 kcal mol^{-1}) was in a good agreement with the experimental enthalpy value of 26 kcal mol^{-1}. Surprisingly, the energy barrier of rotation for (*E,E,E,E*)-[4]CC$_{3,9}$ was[11] so large that no isomerisation occurred even at 473 K over a period as long as 60 d. For a comparison, the half-life of (*E,E,E,E*)-[4]CC$_{2,8}$ was estimated to be 2 s at 453 K and the half-life of rotation around the carbon–carbon double bond with relatively low energy barrier (40 kcal mol^{-1}) is 58 h at 473 K. Such strong constraint at the single-bond linkages shows that (*E,E,E,E*)-[4]CC$_{3,9}$ possesses an extremely persistent tubular shape. Most recently, Isobe and co-workers reported[10] a π-extended derivative of [4]CC$_{2,8}$, namely, [4]CA$_{2,8}$, in which chrysenylene units were replaced by anthanthrenylene units that feature two additional fused benzenoid rings. Similarly to the [4]CC$_{2,8}$ system, six stereoisomers are possible for the [4]CA$_{2,8}$ system (Fig. 5b–d), all of which could be separated and isolated, and some of which also characterised by XRD analysis. This π-extended system displays dynamics similar to that of [4]CC$_{2,8}$, however, the enthalpy barrier of rotation is lower by 5 kcal mol^{-1} compared to the shorter [4]CC$_{2,8}$ system ($\Delta H^{\ddagger}$ = +21 kcal mol^{-1}, $\Delta S^{\ddagger}$ = −15 cal K^{-1} mol^{-1}, $\Delta G_{393}{}^{\ddagger}$ = +27 kcal mol^{-1}).

The bottom-up approach towards CNTs has so far been successful in terms of development of efficient syntheses towards nanoring fragments of CNTs, including chiral ones. The synthesis of nanobelt fragments of CNTs has not yet been achieved and remains[2] as one of the future challenges. The pioneering work revolving around the synthesis of chiral nanorings, however, holds promise for expanding this synthetic methodology to chiral nanobelt structures that are prone towards racemisation even at higher temperatures, as they do not contain single-bond linkages. Such chiral nanobelts can serve as monomer units for polymerisation and ultimately afford enantiopure and structurally uniform chiral CNTs of choice.

3. Chirality in systems with non-zero Gaussian curvature

As stated above, a planar sheet of graphene composed solely of six-membered benzenoid rings can be bent and fused into a tube. The resulting tubular structures represent surfaces of zero Gaussian curvature. When other than six-membered rings are embedded into the hexagonal array of planar sp^2-carbon lattice, causing structural 'defects', surfaces that display positive or negative Gaussian curvature are obtained. Before analysing chirality of these systems, we first illustrate how positive and negative curvature can be achieved in all-sp^2-carbon-based molecules, by using [n]circulenes[14] (Fig. 6) as model structures. [n]Circulenes belong to the class of polycyclic aromatic hydrocarbons (PAHs), which feature a central n-sided polygon (n > 2) fully surrounded by fused six-membered benzenoid rings. Four types of [n]circulenes can be recognised[14] (Fig. 17): positively curved (n = 3–5), planar (n = 6), negatively curved (n = 7–16) and helical (n > 16).

bowl	**disc**	**saddle**
[n] = 3[a]–5	[n] = 6	[n] = 7–16[a]

[4]circulene	[5]circulene	[6]circulene	[7]circulene	[8]circulene
rigid / RSE	non-rigid / RSE	rigid / RSE	fluctuating / no RSE	fluctuating / RSE

Fig. 6 (top) *Schematic illustration of surfaces with positive (left), zero (middle) and negative (right) Gaussian curvature and (bottom) structural formulae and perspective and side views of solid-state structures of [n]circulenes (n = 4–8). The central and outside rings of [n]circulenes are highlighted in orange and gray, respectively. In the case of [4]- and [8]circulene, the parent structures have not been made and the substituents of their known derivatives are omitted for clarity. RSE = reflective symmetry element. [a][n]Circulenes with n = 3 and n > 8 remain to be made and [n]circulenes with n > 16 are predicted to adopt unique helical conformations (see Section 4, Fig. 17).*

Positively curved [3–5]circulenes[15,16] possess a central *n*-sided polygon that has less than six sides. Because the values of the internal angles of a polygon with *n* < 6 are smaller than 120°, the polygon causes distortion of the surrounding benzenoid rings and creates strain that forces the planar form to adopt a bowl-shaped geometry. In planar disc-like [6]circulene[17] (coronene), the central polygon is a hexagon, therefore, all internal angles match the ideal value 120°, resulting in a strain-free structure. In negatively curved [7–16]circulenes[18,19], the values of the internal angles of polygons are larger than 120°. Consequently, a polygon with *n* > 6 induces ring strain that forces a planar form to adopt a saddle-shaped geometry. When the number of polygon sides reaches the value *n* = 17, the [*n* > 16]circulenes start to adopt[14] unique helical geometries according to calculations. This last type of [*n*]circulenes is discussed in Section 4 (Fig. 17).

Because of the strained character of positively and negatively curved [*n*]circulenes, their synthesis requires efficient processes that can build-up the strain in a stepwise manner. This synthetic challenge impedes the preparation of curved [*n*]circulenes and to date, only a handful of them, namely, [4]-,[15] [5]-,[16] [7]-,[18] and [8]circulenes,[19] have been made. In terms of symmetry, all positively curved [*n*]circulenes possess RSEs, namely, *n* planes of symmetry, while the lowest-energy conformations of negatively curved [*n*]circulenes either do not (*n* = odd) or do (*n* = even) possess RSEs, according to calculations. Out of [*n*]circulenes that have been made, only [7]circulene has a lowest-energy conformation that does not contain any reflective symmetry elements (RSEs) and only [4]- and [6]circulenes are rigid ([5]circulene is non-rigid, [7]- and [8]circulenes are fluctuating).

Consequently, none of the parent [4–8]circulenes is chiral. In this section, chirality of polyaromatic systems with non-zero Gaussian curvature derived from [*n*]circulenes is discussed.

3.1 Positively curved chiral polyaromatic systems

Positively curved systems are commonly referred to as molecular 'bowls'. When stereochemically rigid, they can be chiral or achiral depending on the fusion pattern, which determines whether they possess RSEs or not, as schematically illustrated in Fig. 7. Rigid chiral bowls can serve as 'endcaps' for chiral capped tubes (capped CNTs) or spheres (fullerenes), but a combination of two bowls that represent a mirror image of one another can also lead to an achiral sphere. Achiral bowls can be extended into chiral bowls, which can be further extended into achiral capped tubes or spheres. Out of three possible positively curved [*n*]circulenes, [5]circulene[16] (corannulene) is the most studied one, with numerous derivatives having been synthesised,[6] including a few that are skeletally chiral. In contrast, only one substituted derivative of [4]circulene has been reported[15] this far (Fig. 6) and [3]circulene has not yet been synthesised. Corannulene can be viewed as a fragment of spherical fullerenes, such as C_{60} (Fig. 8, left), or as an endcap of capped CNTs[20] (Fig. 10a). Because it has a C_{5v} symmetry, that is, it contains five symmetry planes (RSEs), it is achiral.
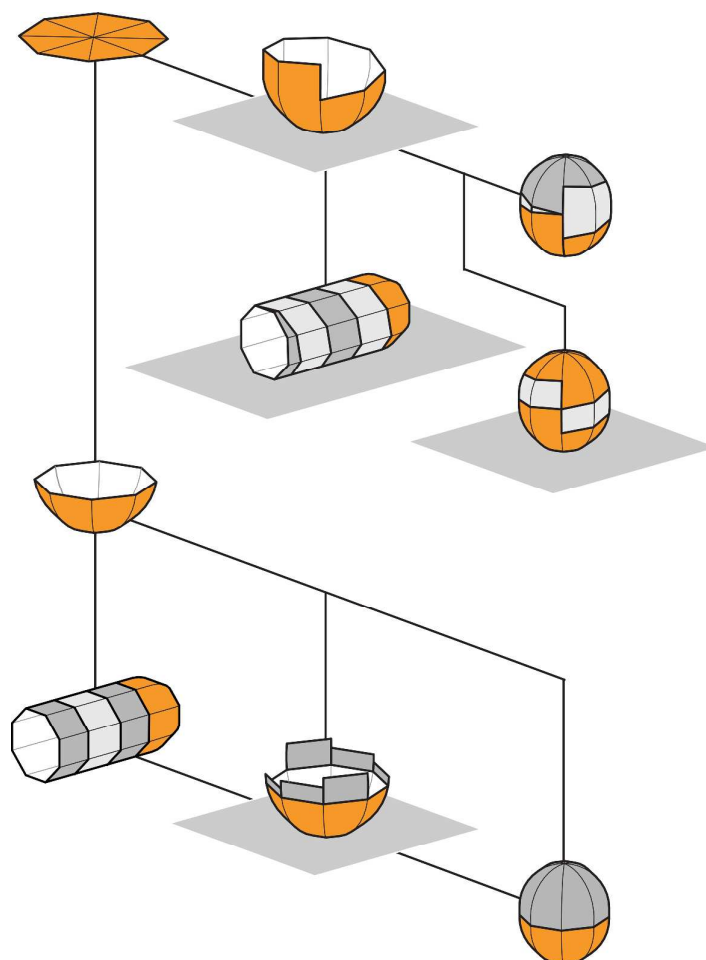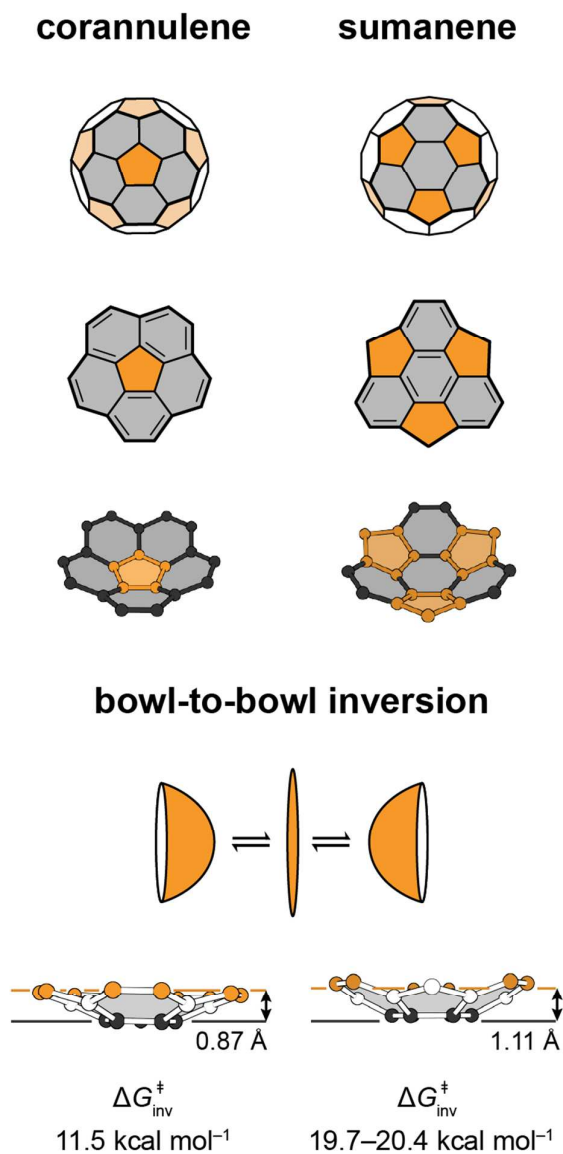
Fig. 7 *Schematic illustration of a transformation of a planar disc (orange, top left) into a chiral and an achiral rigid bowl with positive Gaussian curvature and their transformations into chiral/achiral tubes and spheres. Parent bowls are highlighted in orange, extensions are shown in gray and chiral bowls, tubes and spheres are marked with gray underlying squares/rectangles.*

The smallest fragment of C_{60} with a C_{3v} symmetry is sumanene[21] (Fig. 8), which comprises a central six-membered ring surrounded by three five- and three six-membered rings fused in an alternating fashion. Sumanene contains three symmetry planes (RSEs) and, similarly to corannulene, it is achiral. An intriguing dynamic feature of bowl-shaped systems, such as corannulene and sumanene, is that they undergo bowl-to-bowl inversion (Fig. 8) through a planar or an 'S'-shaped transition state. The energy barrier of this process increases roughly with an increasing bowl depth, here defined (Fig. 8)

as a distance between the best plane of the hub carbon atoms (black; corannulene (five), sumanene (six)) and the best plane of the rim carbon atoms (orange; corannulene (10), sumanene (six)) of the corannulene/sumanene segments. Because corannulene contains one and sumanene three five-membered rings that induce ring distortions, corannulene has a lower bowl depth (0.87 Å) than sumanene (1.11 Å). Accordingly, the value of the Gibbs free energy barrier ($\Delta G^{\ddagger}$) for bowl-to-bowl inversion of sumanene[22] (19.7–20.4 kcal mol^{-1} at 318 K, solvent-dependent) is higher than the value (11.5 kcal mol^{-1}) extrapolated[23] for corannulene. These values imply that corannulene is stereochemically non-rigid and sumanene is at the transition between rigid and non-rigid. In the case of bowl-shaped molecules that do not possess any RSEs, the bowl-to-bowl inversion is a process that converts either (1) one enantiomer to another if one stereogenic unit is present, or (2) one diastereomer to another if more than one stereogenic units are present. Stereochemical rigidity in terms of the bowl-to-bowl inversion (energy barrier >20 kcal mol^{-1}) under ambient conditions is therefore crucial for designing chiral molecular bowls.
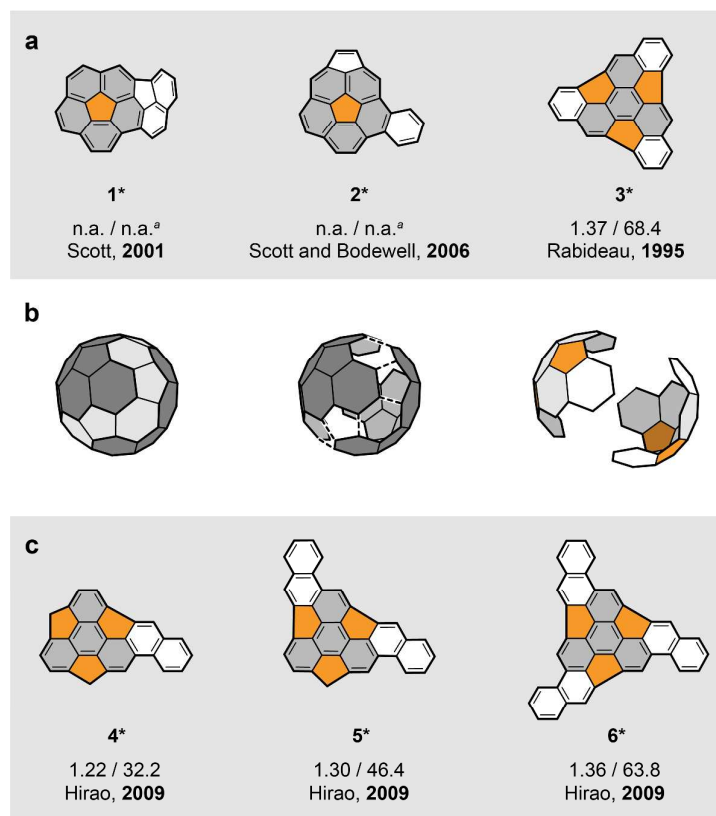
To assure that derivatives based on corannulene and sumanene are chiral, (1) the energy barrier of bowl-to-bowl inversion needs to match the criterion for a stereochemically rigid molecule and (2) the symmetry must be reduced such that the molecule does not contain any RSEs. Because the scope of this tutorial is skeletal chirality of polyaromatic systems, examples where chirality is achieved by peripheral substitution or hetero-doping[24] (replacement of some carbon atoms by other elements, for example, nitrogen atoms), which break the C_{nv} symmetry, fall beyond the scope of this review. Chiral examples of skeletally chiral bowl-shaped molecules that have been described are limited and the most representative examples are discussed below.

corannulene   **sumanene**

bowl-to-bowl inversion

0.87 Å   1.11 Å

$\Delta G^{\ddagger}_{inv}$ $\Delta G^{\ddagger}_{inv}$

11.5 kcal mol^{-1} 19.7–20.4 kcal mol^{-1}

Fig. 8 (top) Schematic illustrations, structural formulae and solid-state structures of corannulene (left) and sumanene (right), bowl-shaped fragments of spherical C_{60}. Colour code: six-membered rings (gray), five-membered rings (orange). (bottom) Schematic illustration of the bowl-to-bowl inversion process and respective energy barriers ($\Delta G^{\ddagger}_{inv}$) of corannulene (extrapolated value) and sumanene (range of experimental values obtained in different solvents).

Two C_1-symmetric derivatives of corannulene (**1** and **2**) are shown in Fig. 9a. Compound **1**[25] features one five- and two six-membered rings and compound **2**[26] one five- and one six-membered rings, fused to the corannulene core. In both cases, the additional rings are fused such that the bowl-shaped conformations do not possess any RSEs and, consequently, both **1** and **2** have C_1 symmetry.

Both compounds can be viewed as π-extended corannulenes or, alternatively, as π-subtracted fullerenes C_{60} or π-subtracted endcaps of capped (5,5)-CNT (Fig 10, top). The values of the bowl depth and the Gibbs free energy barrier for the bowl-to-bowl inversion of **1** and **2** have not been reported. In both cases, however, values similar (**2**) or higher (**1**) than those[27] of cyclopentacorannulene (corannulene-segment bowl depth = 1.09 Å, energy barrier of bowl-to-bowl inversion = 27.6 kcal mol^{-1} at 325 K), an achiral segment of **1** and **2**, can be expected. Based on these anticipated values, **1** and **2** fulfil the criteria of a chiral compound. It should thus be possible to resolve compounds **1** and **2** into enantiomers, although racemisation via bowl-to-bowl inversion can be expected to occur in the order of days/weeks under ambient conditions.


a

1*	**2***	**3***
n.a. / n.a.^{a}	n.a. / n.a.^{a}	1.37 / 68.4
Scott, **2001**	Scott and Bodewell, **2006**	Rabideau, **1995**

b

c

4*	**5***	**6***
1.22 / 32.2	1.30 / 46.4	1.36 / 63.8
Hirao, **2009**	Hirao, **2009**	Hirao, **2009**

*Fig. 9 (a,c) Structural formulae, bowl depths (in Å, number on the left) and energy barriers of bowl-to-bowl inversion (in kcal mol^{-1}, number on the right) of chiral^a bowl-shaped compounds **1–6**. Colour code: five- and six-membered rings of corannulene/sumanene segments (orange and gray, respectively), rings extending the structure of corannulene/sumanene (white). (b) Schematic illustration of 'splitting' fullerene C_{60} into two halves: one (P)- and one (M)-enantiomer of*

*hemifullerene **3**. Chiral systems, that is, rigid systems that do not possess any reflective symmetry elements (RSEs), are highlighted with a gray background and an asterisk next to the compound number. [a]Values similar (**2**) or higher (**1**) than those of cyclopentacorannulene (1.09 / 27.6), an achiral segment of **1** and **2**, are expected. Although none of **1–6** has been separated into enantiomers, they are all anticipated to be chiral (see the discussion in the text).*

Fusing one, two or three benzenoid rings in the cove regions of the sumanene core (periphery sections in between five- and six-membered rings) leads to structures that are chiral, that is, stereochemically rigid and with no RSEs. An example of such π-extended sumanene, tribenzosumanene **3**, is shown in Fig. 9a. Compound **3**, commonly referred[28] to as hemifullerene, is C_3-symmetric and its carbon skeleton represents one half of fullerene C_{60}. Because the two 'halves' of C_{60} are mirror images of one another, C_{60} can be viewed as a racemic conjugate of (*P*)-**3** and (*M*)-**3** (Fig. 9b). The sumanene-segment bowl depth of **3** obtained from its solid state structure is 1.37 Å, 0.26 Å deeper than that of parent sumanene, and the bowl-to-bowl inversion (racemisation) energy barrier estimated[29] by DFT calculations (B3LYP/6-31G(d)) is 68.4 kcal mol^{-1}. The energy barrier value indicates that **3** is stable against racemisation at room temperature, nevertheless, the enantiomers of **3** or its substituted derivatives have not yet been separated and isolated. Structures analogous to **3** can be obtained by fusing naphthalene units in the cove regions of the sumanene core and the corresponding structures of mono- (**4**), di- (**5**) and trinaphthosumanene (**6**)[30] are shown in Fig. 9c. This series illustrates well how fusion of each additional naphthalene unit increases the sumanene-segment bowl depth and, consequently, also the bowl-to-bowl inversion (racemisation) energy barrier: **4** (1.22 Å, 32.2 kcal mol^{-1} (NMR, 140 °C, mesitylene-d_{12}), 31.4 kcal mol^{-1} (DFT/B3LYP/6-31G(d,p)), **5** (1.30 Å, 46.4 kcal mol^{-1} (DFT/B3LYP/6-31G(d,p)) and **6** (1.36 Å, 63.8 kcal mol^{-1} (DFT/B3LYP/6-31G(d,p)). Similarly to **3**, none of the compounds **4–6** have been resolved into enantiomers. Based on the experimental value for the bowl-to-bowl inversion of **4**, however, all compounds **3–6** can be safely regarded as chiral. With regards to their structural relationship to sp^2-carbon allotropes, compounds **3–6** can be viewed as π-extended sumanenes or, alternatively, π-subtracted fullerenes C_{60} or π-subtracted endcaps of capped (6,6)-CNT[7] (Fig 10, middle).

24

Bowl-shaped and stereochemically rigid endcaps of achiral CNTs, for example, (5,5)-CNT endcap[20] based on corannulene (Fig. 10, top) and (6,6)-CNT endcap[7] based on sumanene (Fig. 10, middle), can serve as templates for growing[7] uniform CNTs. To date, however, no bowl-shaped endcaps of chiral CNTs have been synthesised. A theoretical example of an endcap of chiral (7,6)-CNT is given in Fig. 10, bottom. This endcap is a rigid π-extension of a non-rigid molecular bowl derived from sumanene, where one five- and one six-membered ring was replaced by one six- and one seven-membered ring, respectively. As a result, the corresponding endcap is helically chiral (the reader can follow an oligo(paraphenylene) helical path of C[5]PP[2]A nanoring fragment (dark gray) starting from the most outside ring of this endcap in the anticlockwise direction; Fig. 10, bottom). Such chiral endcaps represent alternatives to chiral nanobelts, which can find use in bottom-up construction of chiral CNTs.
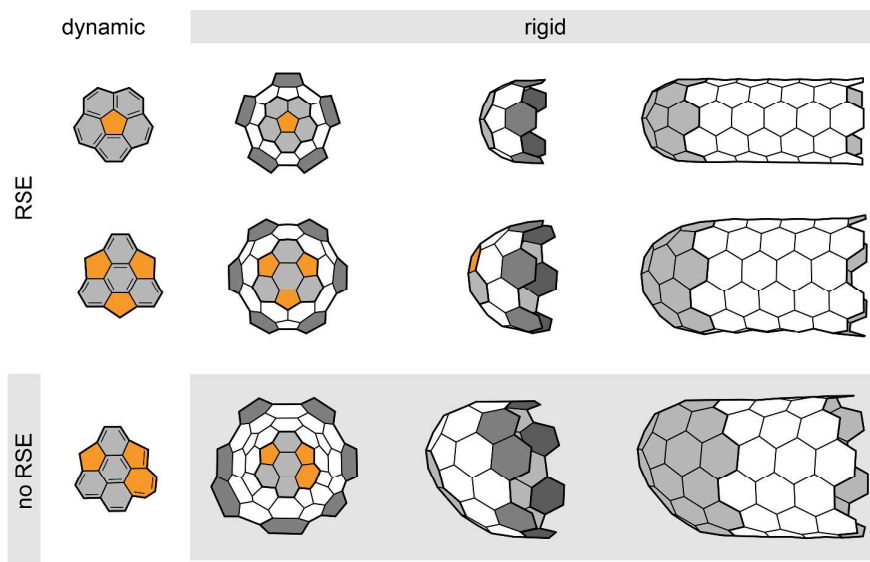
Fig. 10 (left) *Structural formulae of dynamic bowls: (top) corannulene, (middle) sumanene and (bottom) a hypothetical bowl related to sumanene.* ***(centre)*** *Front and side views of rigid CNT endcaps obtained by π-extension of structures on the left.* ***(right)*** *Capped CNTs obtained by π-extension of the endcaps: (top) (5,5)-CNT, (middle) (6,6)-CNT and (bottom) (7,6)-CNT. Five-/seven- and six-membered rings of the bowl segments are highlighted in orange and light gray, respectively. The [5]CPP (top), [6]CPP (middle) and C[5]PP[2]A (bottom) segments of endcaps are highlighted in*

dark gray. The endcap segments of capped CNTs (right) are highlighted in light gray. Chiral systems, that is, rigid systems that do not possess any reflective symmetry elements (RSEs), are highlighted with a gray background.

Examples of stereodynamic (non-rigid/fluctuating) systems based on corannulene that possess more than one stereogenic unit are shown in Fig. 11. Biscorannulene **7**[31] is comprised of two corannulene segments linked via a single bond, a system where three stereogenic axes are present: two are associated with two monosubstituted corannulene units and one is associated with 1,1'-binaphthyl unit. The presence of three stereogenic axes gave rise to a rich stereodynamic system combining twists and curves, where multiple conformers that do not contain RSEs co-exist in equilibrium. To distinguish between all possible conformers, chirality arising from the curvature of each bowl was denoted[31] as *P* or *M*, and chirality related to the C2–C1–C1'–C2' torsion angle (ϕ) of 1,1'-binaphthyl unit was denoted as *R* ($-180° < \phi < 0°$) or *S* ($0° < \phi < 180°$). Six basic conformers include three pairs of enantiomers: (*R,M,M*)/(*S,P,P*), (*R,P,P*)/(*S,M,M*) and (*R,M,P*)/(*S,P,M*). Additionally, each of the six basic conformers has two stable conformers, one in the region $0° < \phi < 90°$ (or $-90° < \phi < 0°$) and one in the region $90° < \phi < 180°$ (or $-180° < \phi < -90°$), therefore, a total of 12 conformers are possible. The DFT calculations (PBE0/6-31G(d)) were used to estimate[31] the energy barriers related to three distinct processes of interconversion between the conformers: steric-hindrance σ-bond rotation barrier ($\phi \sim 0°$ or 180°, 12.9–19.8 kcal mol^{-1}, values significantly lower than those for 1,1'-binaphthyls), bowl-to-bowl inversion barrier (8.7–10.5 kcal mol^{-1}, values similar to those of monosubstituted corannulenes) and conjugation-loss σ-bond rotation barrier ($\phi \sim 90°$, 1–2 kcal mol^{-1}, values similar to those for 1,1'-biphenyls). In accord with the calculated energy barrier values, one set of signals was observed in the ^{1}H NMR spectrum acquired at room temperature, indicating that interconversion between the diastereomeric conformers was fast relative to the NMR time-scale. At 180 K, three sets of signals corresponding to the three possible diastereomeric conformers were observed, indicating slow interconversion relative to the NMR time-scale. Note that bowl-to-bowl inversion alone is sufficient for interconversion between diastereomeric conformers and both the

steric-hindrance σ-bond rotation and bowl-to-bowl inversion need to be slowed down relative to the NMR time-scale for observation of all diastereomeric conformers. The conjugation-loss σ-bond rotation remains fast relative to the NMR time-scale even at 180 K, and each diastereomeric conformer therefore appears as an average of two possible conformations. In the single crystal, the (*R,M,M*)/(*S,P,P*) and (*R,M,P*)/(*S,P,M*) diastereomeric conformers were present in a 7:3 ratio, each as a 1:1 mixture of two enantiomeric conformers, in accord with the calculated ratio corrected for the crystallisation temperature (note that at room temperature in the gas phase, (*R,M,M*)/(*S,P,P*) and (*R,P,P*)/(*S,M,M*) conformers have similar energies, while the (*R,M,P*)/(*S,P,M*) conformer is ~1 kcal mol^{-1} higher in energy). Based on these results, compound **7** can be classified as stereochemically non-rigid and therefore achiral. A similar system was obtained[32] by linking two sumanenes via a single bond to form stereochemically non-rigid bissumanene. Also in this case, a single set of signals was observed in the ^{1}H NMR spectrum at room temperature. This observation can be explained by (1) the presence of a single diastereomeric conformer if steric-hindrance σ-bond rotation is slow relative to the NMR time-scale or (2) the presence of either (*R,M,M*)/(*S,P,P*) and (*R,P,P*)/(*S,M,M*) or (*R,M,P*)/(*S,P,M*) diastereomeric conformers if steric-hindrance σ-bond rotation is fast relative to the NMR time-scale. Note that bowl-to-bowl inversion of sumanene, which is considerably higher than that of corannulene, is slow relative to the NMR time-scale at room temperature.

A unique example of π-extended corannulene is cyclotriscorannulyne **8**[33] (Fig. 11), where three corannulenes are fused to a central six-membered ring. This fusing mode generates three [5]helicene subunits that force the planar D_{3h}-symmetric form to adopt a non-planar structure on account of steric interactions. Compound **8** belongs to the class of D_{3h} overcrowded systems featuring three 'blades', which due to steric congestion adopt either a propeller (up-down-up-down-up-down) or a twisted (up-down-up-up-down-down) conformation. Because the corannulene units are curved, more than these two basic conformations are possible in the case of **8** and the most stable conformation according to calculations (B97-D/TZVP) is also the one that was observed in the solid state (Fig. 11). An intriguing feature of this system is that each corannulene bowl displays[33]

distinctly different energy barrier of bowl-to-bowl inversion: 'up-down' bowl A (8.4 kcal mol^{-1}), 'up-up' bowl B (13.8 kcal mol^{-1}) and 'down-down' bowl C (17.3 kcal mol^{-1}). In addition, the bowl-to-bowl inversion of bowl A leads to an identical structure (pseudorotation), while inversion of bowls B and C affords diastereomeric conformers that are higher in energy by 11.2 and 16.5 kcal mol^{-1}, respectively. The ^{1}H NMR spectrum of **8** acquired at 168 K features 24 signals, as expected for a single diastereomer when bowl-to-bowl and helix inversions are slow relative to the NMR time-scale. At 273 K, the number of resonances is reduced to 12, indicating that inversion of bowl A is fast, while inversions of bowls B and C remain slow relative to the NMR time-scale. At 413 K, the spectrum is simplified to a set of two doublets, consistent with the "ideal" D_{3h} symmetry through the conformational twist-to-twist, twist-to-propeller and/or propeller-to-propeller interconversions. Similarly to **7**, also **8** is stereochemically non-rigid and thus achiral.
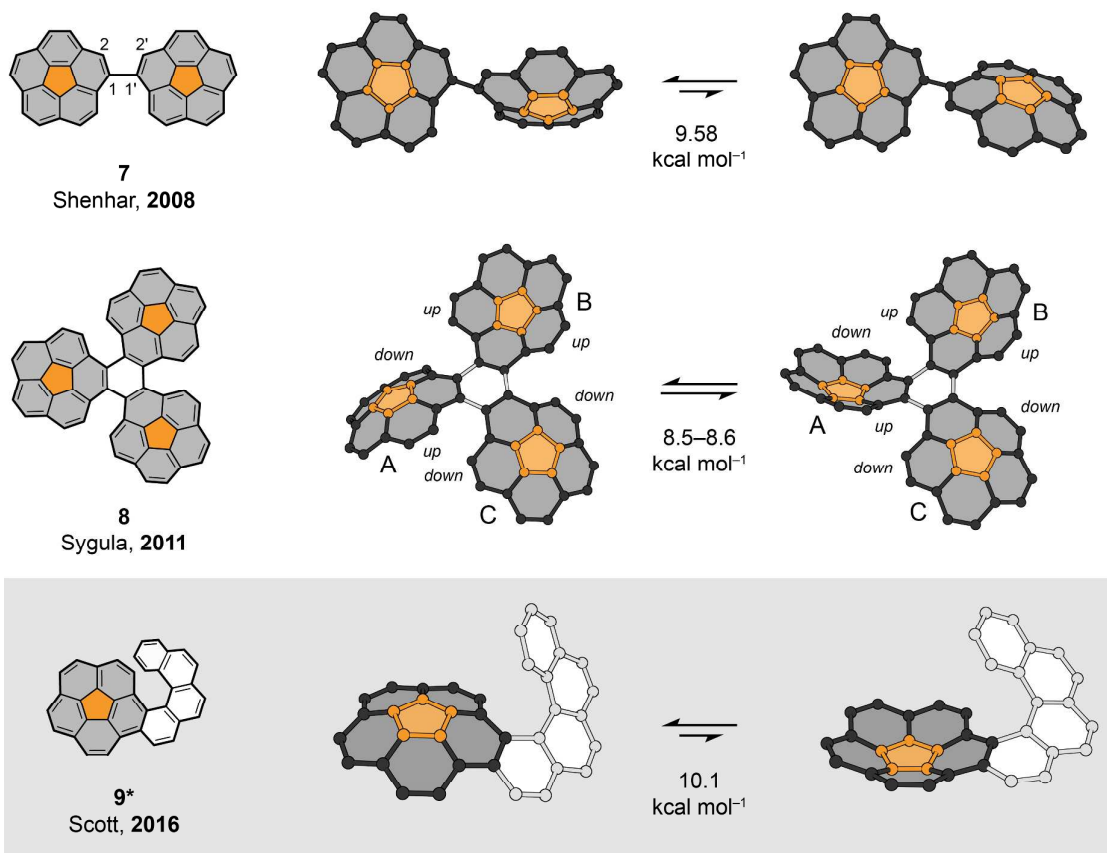
Fig. 11 *Structural formulae of corannulene-based compounds 7–9 (left) and interconversion between selected diastereomeric conformers via bowl-to-bowl inversion: (top) (S,P,P)-7 (XRD) to (S,P,M)-7 (DFT/PBE0/6-31G(d); inversion of right bowl), (middle) pseudorotation of the most stable diastereomeric conformer of 8 (XRD; inversion of bowl A, left and right structures are identical) and (bottom) convex-9 (XRD) to concave-9 (DFT/B3LYP/6-31G(d)). The values of energy barriers for the corresponding processes are given below the arrows. Colour code: five- and six-membered rings of corannulene segment (orange and gray, respectively), additional six-membered rings (white). Chiral system 9, where the [6]helicene unit is stereochemically rigid, is highlighted with a gray background and an asterisk next to the compound number.*

Finally, Scott and co-workers reported two corannulene derivatives, where three and four benzenoid rings are fused to the corannulene core such that they form a [5]- and a [6]helicene unit, respectively. The former system is a segment of compound **8**, while the latter system (**9**)[34] has an extra ring that terminates the [6]helicene unit (Fig. 11). Both compounds possess two stereogenic axes, one associated with the asymmetrically π-extended corannulene unit and one with the helically twisted unit, therefore, they both exist in the form of two diastereomeric conformers, each representing a pair of enantiomeric conformers. The conformers, in which one terminal helicene ring faces the convex surface of the bowl are more stable than those, where the terminal ring faces the concave bowl surface, as the two forms display different degrees of steric congestion (for example, convex-**9** is lower in energy by 6.3 kcal mol^{-1} compared with concave-**9**; Fig. 11). Accordingly, the racemic single crystal contained the enantiomeric conformers of convex-**9** conformer in a 1:1 ratio. Because the bowl and the helix have mutual steric influence on one another, both the bowl-to-bowl and the helix inversion of convex-**9** have lower energy barriers (10.1 and 34.6 kcal mol^{-1}, respectively; 298 K, 1 atm, B3LYP/6-31G(d)) than the parent compounds corannulene (~11.5 kcal mol^{-1}) and [6]helicene (36.2 kcal mol^{-1}). While the diastereomeric conformers can interconvert via either of the processes, enantiomerisation requires both the bowl and the helix inversion. Compound **9** is the first bowl-shaped 'nanocarbon' that was successfully resolved[34] into its enantiomers by using chiral-stationary-phase HPLC. Monitoring of the decrease of enantiomeric excess of an enantioenriched sample over time in 1,2,4-trichlorobenzene allowed

determination of activation parameters of helix inversion ($\Delta H^{\ddagger}$ = 31.5 kcal·mol^{-1}, $\Delta S^{\ddagger}$ = −6.9 cal·mol^{-1}·K^{-1}, $\Delta G^{\ddagger}$ = 33.5 kcal·mol^{-1} at 298 K), which are in consensus with the calculated energy barrier. Compound **9** is an example, where chirality arises on account of the rigid [6]helicene unit and not curvature. As compound **9** contains a non-rigid corannulene unit that undergoes a rapid bowl-to-bowl inversion under ambient conditions, each enantiomer of **9** exists as two diastereomeric conformers undergoing fast interconversion.

The bottom-up synthesis of chiral bowls with positive Gaussian curvature has so far provided systems, where chirality was achieved by π-extension of corannulene and sumanene cores. Some of these chiral rigid bowls best represent fragments of achiral sp^2-carbon allotropes, such as fullerenes and capped CNTs, and can serve as building blocks for their preparation. Other examples include non-rigid systems that possess multiple stereogenic units and display intriguing dynamics of interconversion between possible stereoisomeric conformers. Chiral fragments of chiral sp^2-carbon allotropes, such as the endcap of chiral (7,6)-CNT featuring seven- in addition to five- and six-membered rings (Fig. 10c), have not yet been made and synthetic approaches for making such systems still remain to be developed. A successful synthesis of chiral positively curved endcaps would open up opportunities to access monodispersed chiral fullerenes and CNTs via bottom-up approach. (Note: a review inspecting chirality in fullerenes has recently been reported.[35])

3.2 Negatively curved chiral polyaromatic systems

Out of 10 possible negatively curved [*n*]circulenes (*n* = 7–16), only [7]-[18] and [8]circulenes[19] have been synthesised to date. [7]Circulene is unique in the sense that it is the first member in the [*n*]circulene series, which has a C_2-symmetric saddle-shaped geometry (negative Gaussian curvature) in its most stable conformation, which does not contain any RSEs. Higher homologues (7 < *n* < 17) are predicted to have C_2-symmetric saddle-shaped geometry of their lowest-energy conformations in all cases when *n* is an odd number. The mechanism of interconversion between the two enantiomeric conformers of [7]circulene has not yet been conclusively established, however, recent

theoretical studies[36] indicate that this interconversion might occur through a C_s-symmetric saddle-shaped transition state (Fig. 12a). According to DFT calculations (B3LYP/6-31G(d)), the C_s conformation is higher in energy by 0.05 kcal mol^{-1} compared with the C_2 conformation, and the 'enantiomerisation' process can be viewed as a continuous wave of the seven hexagons, which progresses around the heptagon. A full circle involving several enantiomerisations can be viewed as a 'pseudorotation'. This enantiomerisation pathway has a significantly lower activation barrier compared to the one that proceeds via a planar D_{7h}-symmetric transition state (Fig. 12a) with an activation barrier of 9.0 kcal mol^{-1}. In the case of a related C_2-symmetric saddle-shaped 1,2-dihydro[7]circulene (**10**),[37] an activation-barrier value of 12.2 kcal mol^{-1} was determined experimentally for the saddle-to-saddle inversion by ^{1}H NMR spectroscopy (Fig. 12b).
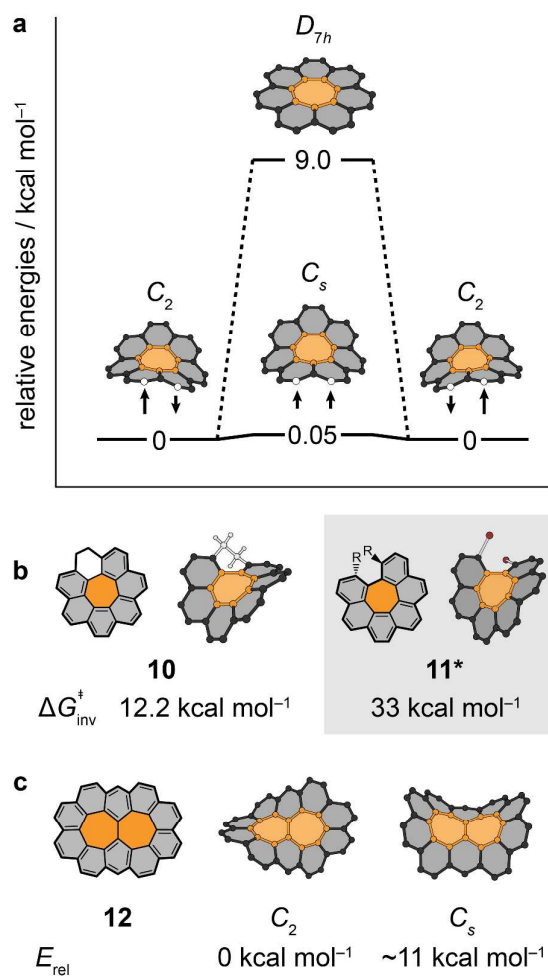
Fig. 12 (a) Energy diagram that illustrates interconversion between the C_2-symmetric saddle-shaped conformers of [7]circulene (XRD) via a curved C_s or a planar D_{7h} transition state (B3LYP/6-31G(d)). (b) Structural formulae of 1,2-dihydro[7]circulene (**10**) and π-subtracted derivatives of [7]circulene, **11a** (R = H) and **11b** (R = Br). Optimised geometry of **10** (B3LYP/6-31G(d,p)) and solid-state structure of **11b** are shown. Energy barriers ($\Delta G^{\ddagger}_{inv}$) of inversion between enantiomeric conformers for **10** and **11b** are given. (c) Structural formula of [7.7]circulene (**12**) and optimised geometries (B3LYP/6-31G(d)) of its C_2 and C_s conformers (their relative energies (E_{rel}) are given). Colour code: seven- (orange) and six-membered (gray) rings, bromine atoms (red). Note: the C_2 symmetry of the C_2 conformer of [7]circulene is better visible in Fig. 6. Chiral system **11** is highlighted with a gray background and an asterisk next to the compound number. Although **11a** is formally achiral ($\Delta G^{\ddagger}_{inv}$ = 17 kcal mol^{-1}), it was separated into enantiomers at low temperatures).

This value is very close to that (12.9 kcal mol^{-1}) estimated by DFT calculations (B3LYP/6-31G(d,p)) for enantiomerisation of **10** via the pseudorotation pathway, supporting the wave-like mechanism for the conformational dynamics of [7]circulene. Based on the activation barriers for the saddle-to-saddle inversion, [7]circulene can be classified as stereochemically fluctuating and **10** as stereochemically non-rigid, and both compounds as achiral. As a result of their dynamic character, [7]circulene and **10** cannot be separated into enantiomers. Nevertheless, [7]circulene represents the smallest [n]circulene as well as the simplest saddle-shaped molecule, the most stable conformation of which does not contain any RSEs.

Removal of a two-carbon edge unit from the parent [7]circulene structure (π-subtraction) gives 1,16-dehydro[6]helicene[18] (or hexa[7]circulene (**11a**), R = H, Fig. 12b), which displays a C_2-symmetric saddle-shaped geometry. Because two hydrogen atoms in the bay region cause steric hindrance, the energy barrier ($\Delta G^{\ddagger}$ = 17 kcal mol^{-1} at 278 K) of interconversion between enantiomeric conformers for this compound is higher than that of [7]circulene. Although this barrier is lower than 20 kcal mol^{-1}, which makes **11a** stereochemically non-rigid and achiral under ambient conditions, **11a** could be resolved into its enantiomers at low temperatures. Even more pronounced increase of the energy barrier ($\Delta G^{\ddagger}$ = 33 kcal mol^{-1} at 412 K) was achieved[18] by introducing two bromine atoms in the bay region (**11b**, R = Br, Fig. 12b), which allowed for the separation of both enantiomers that were stable

against racemisation under ambient conditions. Consequently, compound **11b** represents a chiral derivative of [7]circulene.

A π-extended example derived from [7]circulene is [7.7]circulene (**12**),[38] which features two central seven-membered rings fused together and fully surrounded by 10 fused benzenoid rings (Fig. 12c). The structure of **12** retains the C_2-symmetric saddle-shaped geometry of [7]circulene in its most stable conformation, albeit with a more pronounced helical twist. Although this compound was characterised only by ^{1}H and ^{13}C NMR in solution, our preliminary DFT calculations (B3LYP/6-31G(d)) indicate that its C_2 conformation is lower in energy by about 11 kcal mol^{-1} compared to the C_s conformation (Fig. 12c), which indicates a higher activation barrier for interconversion between enantiomeric conformers compared with [7]circulene. From a stereochemical view, compound **12** can be classified as non-rigid and thus achiral. Combination of two and more seven-membered rings fused together in a row, and surrounded by five- and/or six-membered rings, appears as a suitable structural motif to 'lock' the helical saddle-shaped geometry of [7]circulene. For example, this structural motif can be found in the hypothetical peanut-shaped fullerene dimer shown in Fig. 1e, which is rigid and chiral.

In contrast to [7]circulene, [8]circulene (Fig. 6) has a saddle-shaped geometry with a D_{2d} symmetry. As it contains RSEs, it is achiral. According to calculations,[39] the saddle-to-saddle inversion of [8]circulene proceeds most likely via a wave-like pathway that has a significantly lower activation barrier (2.9 kcal mol^{-1}) than the pathway via planar transition state (125 kcal mol^{-1}, DFT/B3LYP/6-31(d)). Although the parent compound [8]circulene has not yet been prepared, a series of achiral per-substituted derivatives of [8]circulene (**13**, Fig. 13), featuring R (Me or OMe) and Ar (*p*-tolyl or *m*-xylyl) groups, have been reported.[40] The most stable conformation of **13** according to calculations is the one observed in the solid-state structure of **13a** (R = Me, Ar = *p*-tolyl; Fig. 13). Another possible, less stable conformation is one, which is obtained by replacing Ar with R substituents (and vice versa) in the solid-state structure of **13a** shown in Fig. 13. According to calculations, the less stable conformation represents one of the transition states during the saddle-to-saddle inversion of the

more stable conformation, which proceeds with an activation barrier of 15.3 kcal mol^{-1} in the case of

of **13b** (R = Me, Ar = Ph; DFT/B3LYP/6-31(d,p)). This barrier is in a good agreement with an

experimental Gibbs free energy barrier ($\Delta G^{\ddagger}$ = 20.7 kcal mol^{-1} at 443 K) obtained for a more sterically

hindered derivative **13c** (R = Me, Ar = *m*-xylyl).
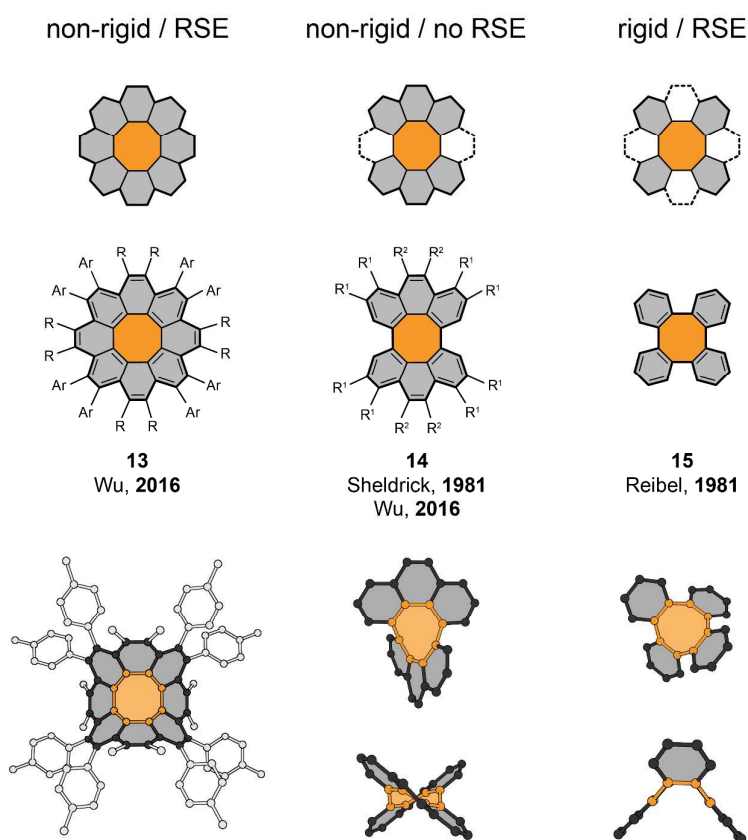
Fig. 13 *(top) Schematic illustration of [8]circulene and its π-subtracted analogues. (middle) Structural formulae of derivatives of [8]circulene (**13a**: R = Me, Ar = p-tolyl; **13b**: R = Me, Ar = Ph; **13c**: R = Me, Ar = m-xylyl) and its π-subtracted analogues (**14a**: R^1, R^2 = H; **14b**: R^1 = Me, R^2 = p-methoxyphenyl; **15**). (bottom) Solid-state structures of **13a**, **14a** and **15**. Colour code: six- (gray) and eight-membered (orange) rings of [8]circulene structure and substructures, p-tolyl rings of **13a** (white). RSE = reflective symmetry element.*

Removal of one to three two-carbon edge units from the parent [8]circulene structure (π-subtraction) can yield saddle-shaped molecules, which have geometry that does not possess any

RSEs on account of steric edge interactions between hydrogen atoms (or substituents) in the formed

bay region. A series of these compounds has been recently prepared. An example of a π-subtracted

[8]circulene short of two two-carbon edge units opposite each other is bis(phenanthrenylene) **14a**[41]

(R^1, R^2 = H; Fig. 13). The parent compound **14a** was reported as early as 1981, however, only its solid-

state structure and not the saddle-to-saddle inversion barrier has been described. Recently, a

persubstituted derivative **14b** (R^1 = Me, R^2 = *p*-methoxyphenyl) analogous to **13** was synthesised[40]

and characterised, for which an experimental value of the Gibbs free energy barrier of saddle-to-

saddle (enantiomerisation) inversion was measured (17.2 kcal mol^{-1}). Based on this value, **14b** can

be classified as stereochemically non-rigid and thus achiral. Removal of four two-carbon edge units

in   an   alternating   fashion   from   the   parent   structure   of   [8]circulene   gives

tetrabenzocyclooctatetraene, or tetra-*ortho*-phenylene[42] (**15**, Fig. 13), that, similarly to [8]circulene,

has an D_{2d}-symmetric saddle-shaped geometry. Its saddle-to-saddle energy barrier has not been

determined experimentally, however, a large activation barrier (of almost 80 kcal mol^{-1}) for

inversion via a non-planar D_4-symmetric transition state has been estimated[43] with the aid of DFT

calculations (B3LYP/6-31G(d,p)). Although **15** is stereochemically rigid, it is achiral as it contains

RSEs, namely, two symmetry planes.

Three examples of π-extended derivatives of [8]circulene and **15** are shown in Fig. 14a.

Tetrabenzo[8]circulene (**16**)[39,44] features four benzenoid rings fused to the [8]circulene core in an

alternating fashion. According to DFT calculations[39] (DFT/B3LYP/6-31G(d)), the most stable

conformers of **16** in the gas phase are **16a** and **16c**, both of which have a D_{2d}-symmetric saddle-

shaped geometry. Compared with **16c**, conformer **16a** is more stable by 5.1 kcal mol^{-1} and

interconverts to **16c** via a pseudorotation pathway involving a S_4-symmetric transition state with an

activation barrier of 7.3 kcal mol^{-1}. The geometry of the transition state is similar to that of **16a**,

albeit slightly twisted (by 5.1°). Interestingly, the solid-state structure features two S_4-symmetric

conformers of **16** (only one conformer, **16b**, is shown in Fig. 14a), which display a more pronounced

twist (32.1 and 37.4°) compared with the transition-state geometry. The solid-state conformers can

be viewed as the 'snapshots' of the pseudorotation process and their geometry is induced by crystal

packing forces on account of small activation barrier of saddle-to-saddle inversion. Single-point DFT

calculations (M06-2X/6-311G(d,p)) performed on the solid-state geometries indicate that both

conformers are higher in energy by ~1.8 kcal mol^{-1} compared with **16a**. Compound **16** thus

represents a unique example of an achiral system (as it is non-rigid and contains RSEs), where

conformation that does not contain any RSEs can be induced in the solid state as a result of its

'floppy' saddle-shaped geometry.
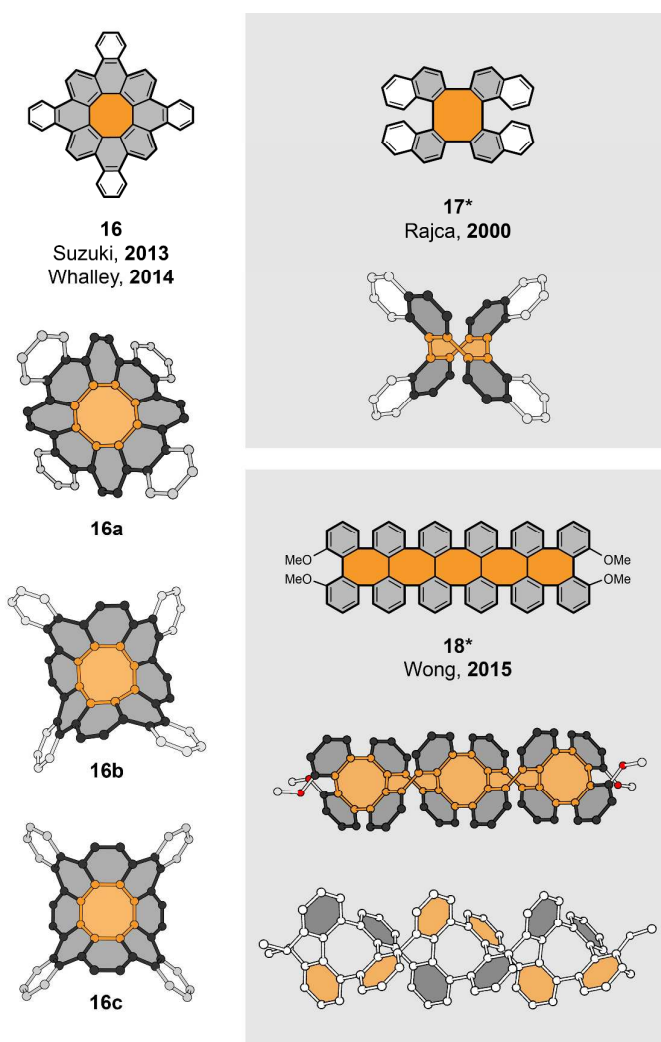
Fig. 14 Structural formulae of **16**, **17** and **18** and their solid-state structures (**16b**, **17** and **18**) and optimised geometries (**16a** and **16c**, DFT/B3LYP/6-31G(d)). Colour code: six- (gray) and eight-

*membered (orange) rings of [8]circulene and tetra-ortho-phenylene units, additional rings (white). The two 'strands' of double-helix structure of **18** are additionally highlighted in orange and gray (bottom left). Chiral systems, that is, rigid systems that do not possess any reflective symmetry elements (RSEs), are highlighted with a gray background and an asterisk next to the compound number.*

π-Extension of the structure of **15** by four fused benzenoid rings is featured in a chiral D_2-symmetric compound **17**[45] (Fig. 14b). Because no appreciable edge interactions are introduced in **17**, the geometry of its tetra-*ortho*-phenylene subunit is almost identical to that of the parent tetra-*ortho*-phenylene (**15**) in the solid state. The structure of **17** comprises two 1,1'-binaphthyl units that have identical configurations linked through the 2- and 2'-positions into a cycle. As **17** is structurally related to **15**, it also exhibits an extremely high saddle-to-saddle inversion (that is, racemisation, in the case of **17**) barrier. Although the exact value of the energy barrier was not determined, the lower limit was experimentally set to 54 kcal mol^{-1} at 613 K (no racemisation was observed when an enantiomerically enriched sample was kept for 14.5 h at 613 K). An intriguing π-extended chiral structure is obtained upon fusing two skeletons of achiral **15** via an additional eight-membered ring. The largest system of this kind (**18**), featuring five tetra-*ortho*-phenylene subunits, have been recently synthesised[46] and characterised both in solution and solid state (Fig. 14c). The structure of **18** can alternatively be described as two oligo-*meta*-phenylene chains (highlighted in orange and gray in Fig. 14c, bottom right) helically wrapped around each other, forming a 'double helix', and linked to form tetra-*ortho*-phenylene subunits. This unique arrangement resembles the double-helix structure of DNA and represents a segment of an achiral sp^2-carbon allotrope proposed[46] by Riley. Although the energy barrier for the helix-to-helix inversion has not been determined experimentally, **18** is expected to be stable against racemisation as in the case of **15** and **17**, and can therefore be categorised as chiral.

This far, chiral structures that display positive or negative Gaussian curvature on account of structural 'defects' in the form of either five-, seven- or eight-membered rings embedded into a hexagonal lattice have been discussed in Section 3. The combination of differently sized rings other

than six-membered rings (for example, five- and seven-membered rings) can also provide a structure with curved geometry. Two representative examples of such systems are shown in Fig. 1 (e and f), where the combination of five- and seven-membered rings is used to conceptualise unique peanut-shaped and toroidal sp^2-carbon structures, the former one being chiral. It is important to note, however, that not all combinations must necessarily lead to a curved geometry, if the ring distortions induced by different rings are cancelled out. Two examples **19**[47] and **20**[48] based on the structure of **15** are given in Fig. 15, in which additional four five- and two four-membered rings cause planarity, as evident from the optimised geometry (DFT/B3LYP/6-31G(d)) of **19** and solid-state structure of **20**.

19
Reiff, **1970**

20
Rajca, **1996**
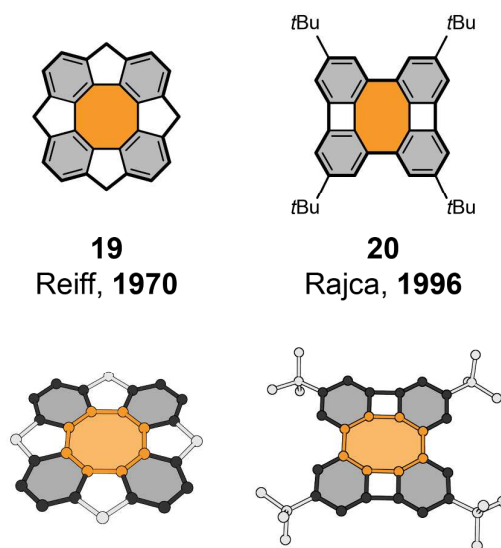
Fig. 15 *Structural formulae of planar **19** and **20**, and optimised geometry (DFT/B3LYP/6-31G(d)) of **19** and solid-state structure of **20**. Colour code: six- (gray) and eight-membered (orange) rings of tetra-ortho-phenylene substructure, additional four- and five-membered rings (white).*

A more 'fortunate' (in the context of this review) combination of five-, six- and seven-membered rings have been designed by Miao and co-workers, who synthesised[49] the largest examples of saddle-shaped molecules to date (**21** and **22**, Fig. 16). Compound **21** possesses two five- and two seven-membered-ring defects that force the entire system to adopt a saddle-shaped geometry. The geometry of **21** contains RSEs, therefore, **21** is achiral. The structure of compound **22** is similar to

that of **21**, except for two five-membered rings that are not present in **22**. As a result, two

[4]helicene subunits emerge in **22**, which force the system into a helical twist (no RSEs). Although

both compounds represent interesting systems for investigating saddle-to-saddle or twist-to-twist

inversion dynamics, neither experimental nor theoretical studies that would provide an insight into

the dynamic behaviour of these large saddles have been reported.

21, Miao, **2015**

22, Miao, **2015**

23, Scott and Itami, **2013**
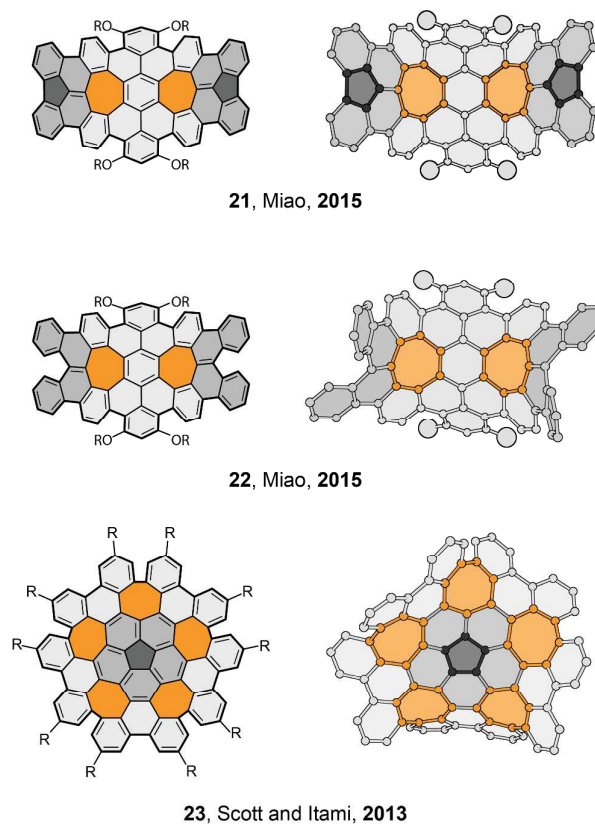
Fig. 16 Structural formulae and solid-state structures of *21–23*. Colour code: five- (dark gray), six-
(semi-dark and light gray) and seven-membered (orange) rings. [4]Helicene and corannulene
subunits are highlighted in semi-dark gray. R = OMe (*21* and *22*) or H/tert-butyl (*23*).

Perhaps the most remarkable non-planar sp^2-carbon sheet has been reported[50] by Scott and Itami.

Their structure, known simply as 'warped nanographene' (**23**, Fig. 16), contains one five- and five

seven-membered-ring defects in the hexagonal lattice. From the standpoint of chemical synthesis, it

is worthwhile to note that the five strained seven-membered rings were formed in a single step. The

structure of **23** features a central bowl-shaped corannulene unit and five hexa[7]circulene moieties (**11a**), each with *P* or *M* configuration around the seven-membered ring. Consequently, two enantiomeric conformers, (*P,M,P,M,P*)- and (*M,P,M,P,M*)-**23**, co-exist in equilibrium. Compound **23** also represents the largest polyaromatic system, other than fullerenes and their derivatives, the structure of which has been determined[50] by X-ray crystallography. It undergoes two distinct dynamic processes, a bowl-to-bowl inversion of the central corannulene unit and enantiomerisation (interconversion between two enantiomeric conformers). The DFT calculations at the B3LYP/6-31G(d) level of theory predict an activation barrier of 1.7 kcal mol^{-1} for the former process and 18.9 kcal

mol^{-1} for the latter. The low energy barrier of bowl-to-bowl inversion is in agreement with the shallow structure of the corannulene unit (bowl depth of 0.37 Å, XRD) and the energy barrier of enantiomerisation is in accord with the experimental value of $\Delta H^{\ddagger}$ = 13.6 kcal mol^{-1} obtained for a decasubstituted derivative of **23**. In terms of curvature, system **23** displays both positive and negative Gaussian curvature. From a stereochemical view, **23** is non-rigid and thus achiral.

In this section, structural defects in the form of non-hexagonal rings introduced in the hexagonal lattice have been analysed in terms of curvature (positive versus negative) and chirality. Based on the variety of examples that were discussed, it becomes clear that embedding of at least one or more seven-membered rings into the sp^2-carbon lattice is a suitable tactic to achieve a curved system that does not contain any RSEs. It, however, remains a challenge to make curved molecules without RSEs that are stereochemically rigid and thus chiral. Understanding structural features that induce chirality of bowl- and saddle-shaped polyaromatic systems is much needed for design of molecular building blocks of sp^2-carbon allotropes with non-zero Gaussian curvature, in particular, negatively curved forms of carbon, such as schwarzite or toroidal nanotubes, which have not yet been made or isolated.

4. Higher circulenes

As mentioned at the beginning of Section 3 (Fig. 6), [*n*]circulenes with *n* > 16 should no longer adopt a saddle-shaped geometry, as a result of steric interactions that arise between opposing rings (see [15]circulene, Fig. 17). Instead, a unique helical geometry is predicted[14] for [17]circulene and its higher homologues (see [18]circulene, Fig. 17), in which the two halves (orange and gray), each representing an oligo-*ortho*-phenylene stripe, are folded around each other in a double-helix manner. Alternatively, each half can be viewed as an [*n*]helicene that wraps around its 'enantiomeric' half. Fig. 17 also shows an energy diagram,[14] in which relative strain energy is plotted against the number of benzenoid rings (or sides of central polygon) of the corresponding [*n*]circulene. From this plot, it is evident that [3]circulene is extremely strained, which is likely the reason why it has not been successfully synthesised. For higher [*n*]circulenes, the strain-energy increase is less steep with increasing *n* and possibly reaches a plateau on account of the helical arrangement. Considering the fact that the largest [*n*]circulene made to date is a derivative of [8]circulene, a beautiful synthetic challenge related to [17]circulene and higher homologues is evident. It is also yet to be discovered whether [*n* > 16]circulenes will be stereochemically rigid and separable into enantiomers under ambient conditions.
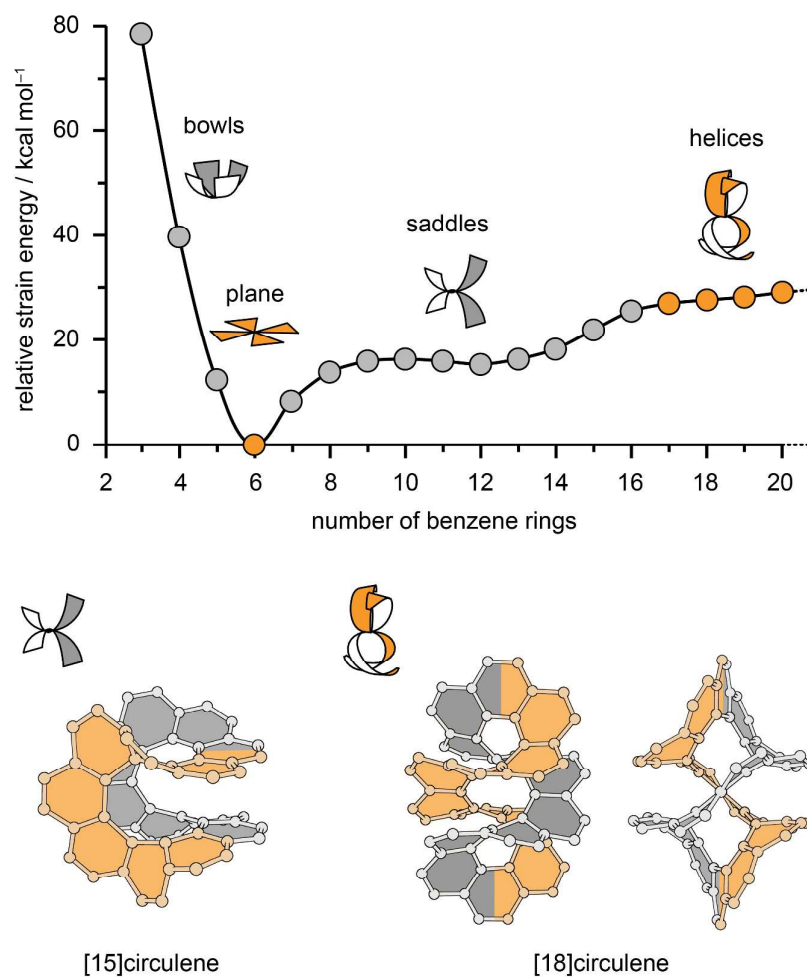
Fig. 17 *(top) Energy diagram, in which relative strain energy of [n]circulenes is plotted against the number of benzenoid rings (or sides of central polygon) that they possess. (bottom) Optimised geometries (DFT/B3LYP/6–31G(d)) of saddle-shaped [15]circulene and 'double-helix' [18]circulene. Two halves of both [n]circulenes are highlighted in orange and gray for clarity.*

5. Conclusion

On account of the practically infinite diversity of structures that can be conceptualised from a single element, natural and synthetic forms of elemental carbon have fascinated scientists for more than a century. Carbon forms constituted of sp^2-hybridised carbon atoms hold a special place in the register of chemists, as they exhibit a broad range of properties that depend strongly on their size and shape. In addition to planar hexagonal arrangements of sp^2-carbon atoms, as in graphene, structural

defects, for example, in the form of non-hexagonal rings, can be introduced in the hexagonal lattice to force a planar structure into a curved geometry. A feature directly related to the symmetry and rigidity of such three-dimensional 'graphenes' is *chirality*. The relationship between the properties and chirality of sp^2-carbon forms, however, goes beyond the rotation of circularly polarised light, as demonstrates the case of carbon nanotubes, where chirality of a given tube dictates its electron-transport ability. In this Tutorial Review, we analysed chiral polyaromatic systems of a finite structure that display zero, positive and negative Gaussian curvature, and which can serve as building blocks for structurally pure and monodispersed allotropic forms of carbon, including hypothetical ones, such as schwarzite. Although a rich variety of chiral curved structures have been reported, particularly in the past decade, their number is still relatively small compared to other classes of chiral compounds, which is mainly due to the synthetic challenge associated with making these highly strained molecules. We hope that the classification and structural analysis of different types of chiral curved polyaromatic systems analysed in this review will inspire future work in this field, including design of new helical motifs, compounds that are stereochemically rigid and prone towards racemisation and their use in construction of new chiral forms of carbon.

6. Available CCDC numbers

(E,E,Z,Z)-[4]CA$_{2,8}$ (927603), tetrabenzo[4]circulene derivative (747755), [5]circulene (1129824), [6]circulene (1129883), [7]circulene (1122356), [8]circulene (1106253), sumanene (266603), **3** (238109), **8** (837369), **11** (1166598), **13** (938414), **14** (1104816), **15** (1106253), **16b** (949624), **20** (1271830), **23** (919707).

7. Optimised geometries

Optimised geometries (DFT/B3LYP/6-31G(d)) of those compounds, which have not been available in the literature, are provided as Electronic Supplementary Information (ESI) PDB files.

8. Acknowledgements

9. References

1   Y. Segawa, H. Ito and K. Itami, *Nat. Rev. Mater.*, 2016, **1**, 1–14 and references cited therein.

2   Y. Segawa, A. Yagi, K. Matsui and K. Itami, *Angew. Chem. Int. Ed.*, 2016, **55**, 2–25 and references cited therein.

3   A. L. Mackay and H. Terrones, *Nature*, 1991, **352**, 762.

4   F. Beuerle, C. Herrmann, A. C. Whalley, C. Valente, A. Gamburd, M. A. Ratner and J. F. Stoddart, *Chem. Eur. J.*, 2011, **17**, 3868–3875.

5   M. V. Diudea, C. L. Nagy, I. Silaghi-Dumitrescu, A. Graovac, D. Janežič and D. Vikić-Topić, *J. Chem. Inf. Model.*, 2005**, 45**, 293–299.

6   *Polycyclic Arenes and Heteroarenes*, Q. Miao, Ed., Wiley-VCH, Weinheim, 2016 and references cited therein.

7   J. R. Sanchez-Valencia, T. Dienel, O. Gröning, I. Shorubalko, A. Mueller, M. Jansen, K. Amsharov, P. Ruffieux and R. Fasel, *Nature*, 2014, **512**, 61–64.

8   M. Rickhaus, M. Mayor and M. Juríček, *Chem. Soc. Rev.*, 2016, **45**, 1542–1556.

9   H. Omachi, Y. Segawa and K. Itami, *Org. Lett.*, 2011, **13**, 2480–2483.

10   T. Matsuno, S. Kamata, S. Hitosugi and H. Isobe, *Chem. Sci.*, 2013, **4**, 3179–3183 and reference 5 cited therein.

11   S. Hitosugi, T. Yamasaki and H. Isobe, *J. Am. Chem. Soc.*, 2012, **134**, 12442–12445.

12   S. Hitosugi, W. Nakanishi, T. Yamasaki and H. Isobe, *Nat. Commun.*, 2011, **2**, 492 and reference 8 (proposed rules for determination of absolute configuration of CNTs) cited therein.

13   P. Sarkar, Z. Sun, T. Tokuhira, M. Kotani, S. Sato and H. Isobe, *ACS Cent. Sci.*, 2016, **2**, 740–747 and references 19, 20 and 22 cited therein.

14   H. Christoph, J. Grunenberg, H. Hopf, I. Dix, P. G. Jones, M. Scholtissek and G. Maier, *Chem. Eur. J.*, 2008, **14**, 5604–5616.

15   Bharat, R. Bhola, T. Bally, A. Valente, M. K. Cyrański, Ł. Dobrzycki, S. M. Spain, P. Rempała, M. R. Chin and B. T. King, *Angew. Chem. Int. Ed.*, 2010, **49**, 399–402.

16   J. C. Hanson and C. E. Nordman, *Acta Cryst.*, 1976, **B32**, 1147–1153.

17   J. K. Fawcett and J. Trotter, *Proc. Royal Soc. Lon. Ser. A*, 1965, 366–377.

18   K. Yamamoto, T. Harada, Y. Okamoto, H. Cbikamatsu, M. Nakazaki, Y. Kai, T. Nakao, M. Tanaka, S. Harada and N. Kasai, *J. Am. Chem. Soc.*, 1988, **110**, 3578–3584.

19   C.-N. Feng, M.-Y. Kuo and Y.-T. Wu, *Angew. Chem. Int. Ed.*, 2013, **52**, 7791–7794.

20   L. T. Scott, E. A. Jackson, Q. Zhang, B. D. Steinberg, M. Bancu and B. Li, *J. Am. Chem. Soc.*, 2012, **134**, 107–110.

21   H. Sakurai, T. Daiko, H. Sakane, T. Amaya and T. Hirao, *J. Am. Chem. Soc.*, 2005, *127*, 11580–11581 and reference 4 cited therein.

22   T. Amaya and T. Hirao, *Pure Appl. Chem.*, 2012, **84**, 1089–1100.

23   T. J. Seiders, K. K. Baldridge, G. H. Grube and J. S. Siegel, *J. Am. Chem. Soc.*, 2001, **123**, 517–525.

24   Q. Tan, S. Higashibayashi, S. Karanjit and H. Sakurai, *Nat. Commun*., 2012, **3**, 891.

25   V. M. Tsefrikas and L. T. Scott, *Chem. Rev.*, 2006, **106**, 4868 and reference 33 cited therein.

26   V. M. Tsefrikas, S. Arns, P. M. Merner, C. C. Warford, B. L. Merner, L. T. Scott and G. J. Bodwell, *Org. Lett.*, 2006, **8**, 5195–5198.

27   A. Sygula, A. H. Abdourazak and P. W. Rabideau, *J. Am. Chem. Soc.*, 1996, **118**, 339–343.

28   M. A. Petrukhina, K. W. Andreini, L. Peng and L. T. Scott, *Angew. Chem. Int. Ed.*, 2004, **43**, 5477–5481.

29   A. Sygula and P. W. Rabideau, *J. Chem. Soc., Chem. Commun.*, 1994, 1497–1499.

30   T. Amaya, T. Nakata and T. Hirao, J*. Am. Chem. Soc.*, 2009, **131**, 10810–10811.

31   D. Eisenberg, A. S. Filatov, E. A. Jackson, M. Rabinovitz, M. A. Petrukhina, L. T. Scott and R. Shenhar, *J. Org. Chem.*, 2008, **73**, 6073–6078.

32   T. Amaya, K. Kobayashi and T. Hirao, *Asian J. Org. Chem.*, 2013, **2**, 642–645.

33   M. Yanney, F. R. Fronczek, W. P. Henry, D. J. Beard and A. Sygula, *Eur. J. Org. Chem.*, 2011, 6636–6639.

34   T. Fujikawa, D. V. Preda, Y. Segawa, K. Itami and L. T. Scott, *Org. Lett.*, 2016, **18**, 3992–3995.

35   C. Thilgen and F. Diederich, *Chem. Rev.*, 2006, **106**, 5049–5135.

36   M. Hatanaka, *J. Phys. Chem. A*, 2016, **120**, 1074–1083.

37   K. Yamamoto, H. Sonobe, H. Matsubara, M. Sato, S. Okamoto and K. Kitaura, *Angew. Chem. Int. Ed. Engl.*, 1996, **35**, 69–70.

38   K. Yamamoto, Y. Saitho, D. Iwaki and T. Ooka, *Angew. Chem. Int. Ed. Engl.*, 1991, **30**, 1173–1174.

39   Y. Sakamoto and T. Suzuki, *J. Am. Chem. Soc.*, 2013, **135**, 14074–14077.

40   C.-N. Feng, W.-C. Hsu, J.-Y. Li, M.-Y. Kuo and Y.-T. Wu, *Chem. Eur. J.*, 2016, **22**, 9198–9208.

41   H. Irngartinger, W. R. K. Reibel and G. M. Sheldrick, *Acta Cryst.*, 1981, **B37**, 1768–1771.

42   H. Irngartinger and W. R. K. Reibel, *Acta Cryst.*, 1981, **B37**, 1724–1728.

43   S. M. Bachrach, *J. Org. Chem.*, 2009, **74**, 3609–3611.

44   R. W. Miller, A. K. Duncan, S. T. Schneebeli, D. L. Gray and A. C. Whalley, *Chem. Eur. J.*, 2014, **20**, 3705–3711.

45   A. Rajca, A. Safronov, S. Rajca and J. Wongsriratanakul, *J. Am. Chem. Soc.*, 2000, **122**, 3351–3357.

46   J.-X. Chen, J.-W. Han and H. N. C. Wong, *Org. Lett.*, 2015, **17**, 4296–4299 and reference 5 cited therein.

47   D. Hellwinkel and G. Reiff, *Angew. Chem. Int. Ed.*, 1970, **9**, 527–528.

48   A. Rajca, A. Safronov, S. Rajca, C. R. Ross and J. J. Stezowski, *J. Am. Chem. Soc.*, 1996, **118**, 7272–7279.

49   K. Y. Cheung, X. Xu and Q. Miao, *J. Am. Chem. Soc.*, 2015, **137**, 3910–3914.

50   K. Kawasumi, Q. Zhang, Y. Segawa, L. T. Scott and K. Itami, *Nat. Chem.*, 2013, **5**, 739–744.

10. Author biographies

Michel Rickhaus obtained his MSc (2011) and PhD (2015) from the University of Basel under the supervision of Professor Marcel Mayor, where he investigated new concepts for inducing twist and strain in aromatic molecules. Under the supervision of Professor Lawrence T. Scott at Boston College, he worked as a visiting scholar on planarisation of curved aromatic systems. Currently, he is

a postdoctoral fellow in the group of Professor Harry L. Anderson at the University of Oxford, constructing three-dimensional porphyrin arrays.

Marcel Mayor received his PhD (1995) from the University of Bern supervised by Professor Rolf Scheffold and Professor Lorenz Walder. After working with Professor Jean-Marie Lehn at the University Louis Pasteur in Strasbourg and at the Collège de France in Paris, he founded his own research group at the Karlsruhe Institute of Technology in 1998. On defending his habilitation in 2002, he became Professor of Chemistry at the University of Basel in 2004. His current research interests are supramolecular chemistry, molecular electronics, nanoscale architectures, functional materials and hybrid materials.

Michal Juríček received his MSc (2005) from Comenius University in Bratislava before he pursued his PhD (2011) at Radboud University Nijmegen with Professor Alan E. Rowan. In 2011, he joined the group of Professor J. Fraser Stoddart at Northwestern University as a postdoctoral fellow. He currently leads an independent research group at the University of Basel, where he investigates polycyclic hydrocarbons with delocalized spin densities.